Mechanical Behavior of Polyurethane Stabilized Fouled Ballast (PSFB)

by

TOLGA DÖLÇEK

A dissertation submitted in partial fulfillment of

the requirements for the degree of

MASTER OF SCIENCE

(GEOLOGICAL ENGINEERING)

at the

UNIVERSITY OF WISCONSIN-MADISON

2014

Mechanical Behavior of Polyurethane Stabilized Fouled Ballast (PSFB)

_____ _____

Students Name Campus ID Number

Approved:

_____ _____

Signature Date Signature Date

James M. Tinjum, Associate Professor Tuncer B. Edil, Professor

DEDICATION

To My Wife and My Son for unconditional love and support.

ABSTRACT

The United State Federal Railway Administration (FRA, 2010) estimates that the demand for rail freight transportation (tonnage) will increase 88% by 2035. North American railroads spend about $3.4 billion every year on track substructure maintenance and renewal due to track-component degradation (Li et al. 2004). These increases in traffic density and weight will cause more deformation and, consequently, more maintenance of the ballast layer. An alternative method in order to decrease maintenance cost is desirable. One such method is injection of polyurethane resin at critical locations in the ballast. This method is effective on clean ballast as a preventive measure (Keene at al. 2012). This study is aimed at evaluating its effectiveness in remediating fouled ballast through polyurethane injection clean ballast was mixed with various types of fouling at different amounts, water contents, and sealed in rectangular (76 mm x 76 mm x 290 mm) and cylindrical (254 mm x 508 mm) molds. The polyurethane was injected into the molds and the specimens were cure for 24 hours. Testing protocol was developed to quantify plastic deformation, flexural strength, and unconfined compressive strength of the fouling ballast stabilized by polyurethane. Average flexural strength of PSB (938 kPa) is about 35% greater than the average flexural strength of PSFB (611 kPa). The average UCS strength of the PSB specimens (3200 kPa) is greater than that of the PSFB specimens (2713 kPa). However, PSFB has a greater strength (about 74%) than unstabilized clean ballast. The PSFB cylindrical specimen with different FI and WC under cyclic loading with deviator stress, σd of 350 kPa, the plastic strains vary between 0.9% - 1.02%, which are under the FRA limit for maintenance (2.5% - 3%) (Hesse, 2013, Keene et al. 2012). The results show that the injection of polyurethane into fouled ballast significantly reduces plastic strain and increases strength. Increasing amounts of fouling material and water content reduces strength and increases plastic strain. Results of this study are then compared with a previous study on clean ballast injected with polyurethane. The use of polyurethane injection into the ballast has the potential to be a fast and cost effective solution for maintenance of the railway systems.

ACKNOWLEDGEMENTS

First and foremost, I would like to express my sincere gratitude to Professors Edil, Tinjum, and Fratta for their kind guidance, excellent interaction, and support in this research.

I want to thank many people who gave me great help and suggestions. Especially I would like to thank Ben Warren, Abdullah Alsabhan and Dr. Ali Soleimanbeigi for their excellent technical advice and assistance in my research.

Finally, I am indebted to my parents for their endless love and boundless mental support and all the members of my family for their encouragement. To my lovely wife, Ayse Ozdogan Dolcek and my little one Emir Salih Dolcek I extend my deepest thanks for exceptional patience, moral support, and sacrifices throughout this research.

Table of Content

List of Figures

List of Tables

DISCLAIMER

This research was funded by the National Center for Freight and Infrastructure Research and Education. The contents of this report reflect the views of the authors, who are responsible for the facts and the accuracy of the information presented herein.

1. INTRODUCTION

According to the Federal Railroad Administration (FRA, 2010), between 1980 and 2008 traffic on Class 1 railroads increased 93% while the length of total track owned decreased 42%, thus leading to a large increase in traffic density. The United State FRA estimates that the demand for rail freight transportation (tonnage) will increase 88% by 2035 (FRA, 2010). The US requires the movement of approximately 40 tons of freight every year and 91% rail freight are bulk commodities, such as agriculture and energy products, automobiles, construction materials, chemicals, coal, equipment, food, metals, minerals, and paper (FRA, 2010). In 2000, Class 1 rail operators in the US spend $500 million each year on ballast maintenance for 150,000 km of Class 1 track (Chrismer and Davis 2000).

Ballast is one of the most important materials used for the structural support of the rail superstructure and leads to distribute loads from the track into the lower substructure layers. Under repeated loading, ballast breaks and broken particles (fouling materials) accumulate in the ballast layer a process that is termed 'fouling'. The fouling material could also come from spillage and mud-pumping of the subgrade or subballast. The fouled ballast (i.e., containing fine particles) can be compromised, thus leading to track instability and, ultimately, train derailments. Seriously fouled ballast defined as having a fouling index of 25% and moisture content of 15% Ebrahimi et al. (2011) is structurally unstable. Since replacing fouled ballast is very expensive in terms of construction equipment, time, and labor force, alternative solutions for consideration and evaluation are essential.

Injection of polymer is a relatively recent and novel method that has been used in various applications of infrastructure remediation. Rigid-polyurethane foam (RPF), which is a high-

density, expanding, thermoset, hydro-insensitive and environmentally neutral polyurethane-resin system, has been used in substructure stabilization. RPF may be appropriate for stabilizing the ballast layer for the following reasons: (1) to reduce ballast particle breakage, (2) to prevent entrance into the ballast layer of fouling materials either from above (spilling) or below (pumping), (3) to fill out voids in ballast to make better contact between the ballast particles, consequently to improve the mechanical properties of the matrix (Keene et al. 2012), and (4) to stabilize and enhance the ballast under the loading (Thomson and Woodward 2004). However, very few experimental and analytical methods have been developed to determine mechanical properties of materials; i.e., ballast stabilized with polyurethane (PSB) and behavior of stabilized track-substructure (Ebrahimi et al. 2011) especially if the ballast is already fouled. Method of polyurethane injection and the effectiveness of polyurethane injection in clean ballast have been investigated at the University of Wisconsin-Madison with positive results (Keene et al. 2012). However, polyurethane stabilization of fouled ballast has not been investigated.

Thus, the objective of this research is to assess the feasibility of strategically placed polyurethane stabilized layers within the ballast structure to mitigate ballast fouling impact and improve the mechanical behavior of fouled ballast.

2. BACKGROUND

2.1 INTRODUCTION

The United State (US) Department of Transportation (DOT) estimates that the demand for rail freight transportation (tonnage) will increase 88% by 2035. Freight is moved by rail, water, pipeline, truck, and air. The rail network accounts for approximately 40% of U.S. freight moves by ton-miles (the length freight travels) and 16% by tons (the weight of freight moved) (see Fig. 2.1). The 91% of rail freight are bulk commodities, such as agriculture and energy products, automobiles and components, construction materials, chemicals, coal, equipment, food, metals, minerals, and paper and pulp (FRA, 2010).

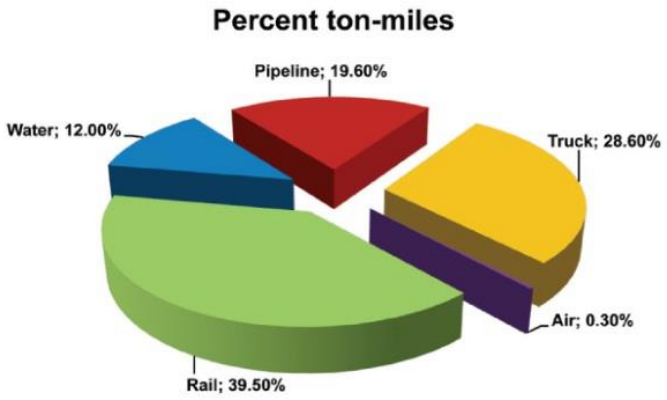

Figure 2.1. Freight Moving Distribution (FRA, 2010)

A railway consists of a superstructure and substructure as shown in Fig. 2.2. The track superstructure receives the load stress from the rolling stock and transmits it to the substructure. Fastening system is to retain the rails against the sleeper and resist vertical and overturning movements of the rail. Sleeper or tie, which is made from wood or concrete receive the load from the rail and distribute it over the supporting ballast and it holds the fastening system to

maintain the proper track gage. The superstructure is supported by a substructure of ballast, subballast, and subgrade. Ballast is usually an angular, uniformly graded, crushed granular material (e.g. granite, dolomite, limestone, slag and gravel) placed at the top of the substructure in which the sleeper is embedded. Angularity of ballast increases friction interlock between grains, which increases the shear strength. Holz and Gibbs (1956) concluded that the shear strength of highly angular materials is higher than that of relatively sub-angular, or sub-rounded metarilas. According to Selig and Water (1994), ballast performs many functions: (1) resisting vertical and lateral forces applied to the sleeper to retain track in its required position, (2) providing large void space for storage of fouling material in the ballast, (3) providing immediate drainage of water falling onto the track, (4) providing some of the resiliency and energy absorption for the track, and (5) reducing pressure from the sleeper bearing area to acceptable stress level for the underlying materials. Subballast is a layer between the ballast and the subgrade and reduces the traffic induced stress at the bottom of the ballast and extends the subgrade frost protection. The most common subballast materials are broadly-graded naturally occurring or processed sand-gravel mixture, or broadly-graded crushed natural aggregates or slag (Selig and Water 1994). The American Railway Engineering and Maintenance of Way Association (AREMA) Engineering Manual specifies a 305 mm as a minimum ballast thickness and a 150 mm as the minimum subballast thickness. This results in a minimum granular layer of 460 mm in rail substructure. The subgrade is the platform upon which the track structure is constructed and main function is to provide a stable foundation for the subballast and ballast.

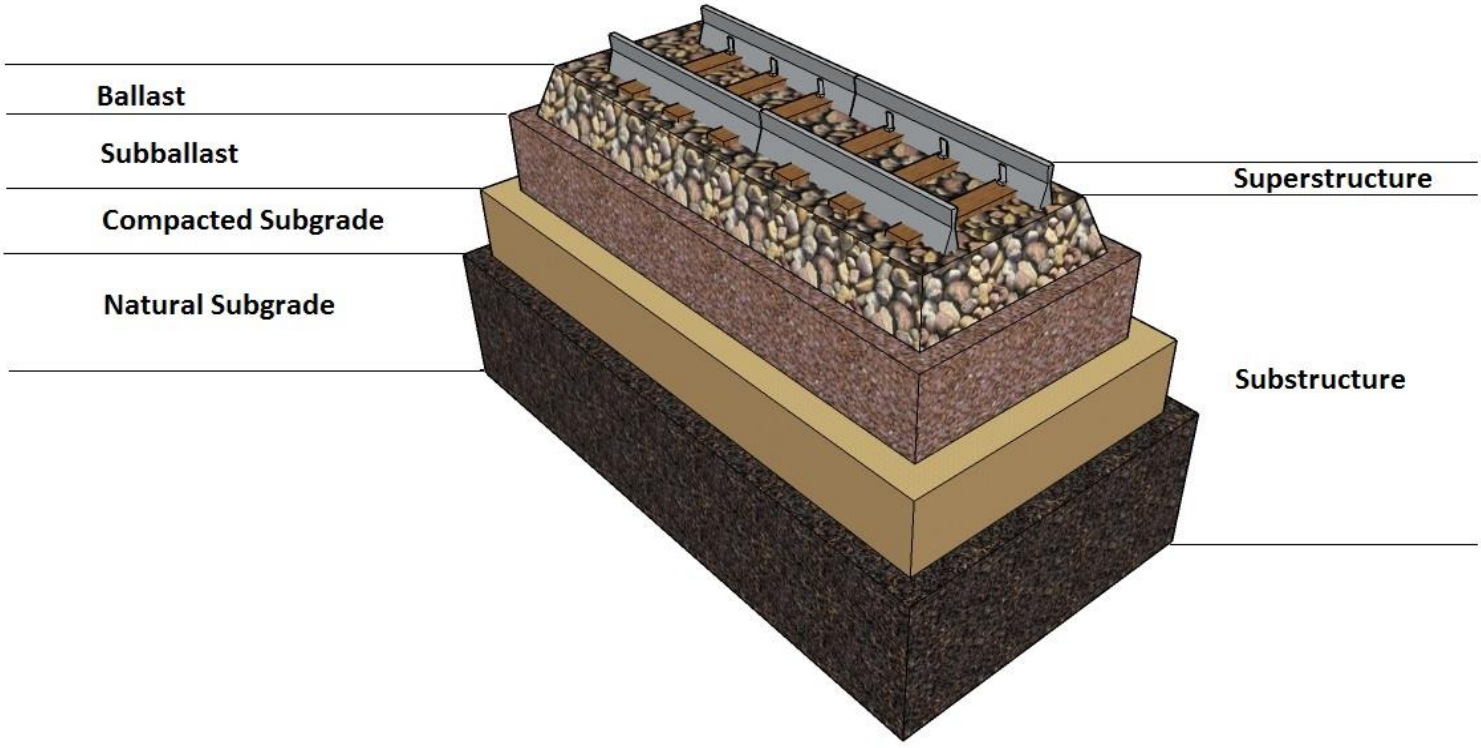

Figure 2.2 Typical Components of Superstructure and Substructure in a Railway Track

Ballast is the most important layer in the rail substructure, and life of the ballast is mainly depends on fouling, i.e. presence of finer-graded materials. The FI is calculated by summing percent particles passing 4.75 mm (P4) and percent particles passing 0.075 mm (P200); hence, (FI=P4+P200) (Selig and Waters 1994). Ballast with a FI between 20% and 39% is considered highly fouled (Ebrahimi et al. 2011). As seen in Fig. 2.3, ballast fouling is generally generated from five different common sources; (1) ballast breakdown from mechanical weathering (freeze-thaw and temperature effects) and tamping as well as from traffic loading, (2) infiltration from ballast surface from car droppings and water or wind, (3) sleeper wear which can be occur from both wood and concrete sleepers, (4) infiltration from underlying granular layers, which is through particle migration into the ballast void because of the pumping action traffic, and (5) subgrade infiltration from clay rich mudstone surface pumps up into the ballast with water. The average percentage by weight of the fouling components for each of the five fouling types was also determined by Selig and Water (1994) and presented in Fig. 2.4.

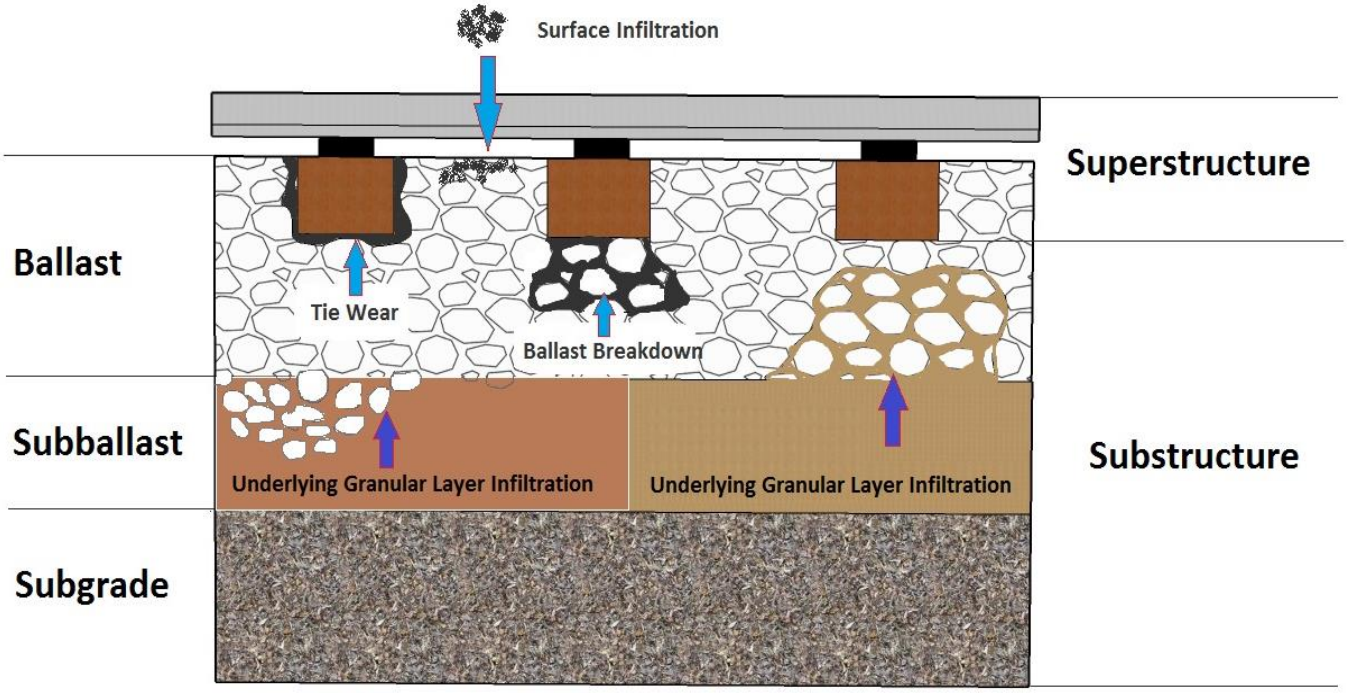

Figure 2.3 Sources of Ballast Fouling in Railway Track (Selig and Waters 1994)

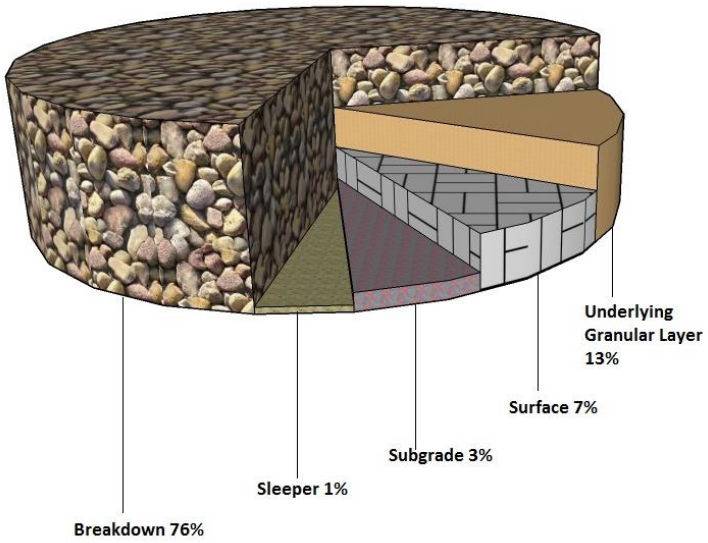

Figure 2.4 The Average Percentage by Weight of the Fouling Components for Each of the Five Fouling Components (after Selig and Water, 1994)

The impacts of ballast fouling depend on the amount and the character of the fouling material. Fouling material amount and size reduce the ballast void space, make the void size smaller and decrease the ballast performance. Furthermore, the amount of water also plays a critical role in ballast performance. When the fouled ballast is wet, the ballast material will be coated with fines and lubricated and the ballast will have weakened structure after traffic load. Fouling impacts the track performance by changing the mechanical properties of substructure layers through (1) loss of effective drainage, (2) formation of "mud-holes", (3) lack of resistance to lateral and longitudinal forces, (4) poor durability after maintenance, and (5) increasing rate of deterioration (Haque et al. 2008; Zaayma 2006; Liu and Xiao 2010). A recent study indicated that as the amount of fouling increases, the strength of the ballast layer decreases, leading to higher rates of track deformation (Ebrahimi et al. 2011). A replacement of the ballast might be needed in the case of highly fouled ballast. However, ballast cleaning and ballast renewal are costly and time-consuming operations, which are disruptive to railway traffic. Ballast renewal consists of 40% of track renewal each year, which consists of 595,000 tons of ballast renewed (Becker and Patrick 2005). North American railroads spend about $3.4 billion every year on track maintenance and renewal due to track-component degradation (Li et al. 2004).

In this study rigid polyurethane foam (RPF) injection method have been evaluated for increasing mechanical properties and lifecycle characteristics of already fouled ballast and for decreasing maintenance costs. RPF is a two-liquid component, which are polyester or polyether polyol and organic polyisocyanate, high-density, closed cell, thermoset, hydrophobic, expanding, polyurethane-resin system. Polyurethane has been used many different industries (see Table 2.1). In the automotive industry, flexible and semi-flexible polyurethane foams have been used extensively for interior components of automobiles, in seats, headrests, armrests, roof liners,

dashboards and instrument panels. Rigid-compact polyurethane desired shape and size for use in a variety of furniture and furnishings applications. The footwear industry replaces materials traditionally used for shoe manufacturing, such as leather and padding, with polyurethane for wear resistant characteristics (Randall and Lee 2002). The construction industry uses a variation of a semi-rigid-foam polyurethane (i.e., thermoset foam) for insulation properties due to the closed-cell, low thermal conductivity, and lightweight properties. RPF have been used to support strength of the construction materials and it has been generally used in structural applications because of high strength, light weight and quick setting processes. Freitas et al. (2010) conducted a parametric study on the use of rigid-foam polyurethane in an experimental orthotropic steel bridge deck for reducing bridge weight for long span and movable bridge applications. In Freitas et al. (2012), the objective was to study the reduction in the direct stress carried to the top plate from vertical loading and increase the stiffness of the bridge section. Erdemgil et al. (2007) investigated the effect of injecting rigid-foam polyurethane beneath a building for mitigating seismic foundation failure from earthquakes. Erdemgil et al. (2007) reported that the SPT blow count before the subsurface injections were 10 to 25 for the clayey-sand and 8 to 14 for the silty-sand layer; after the subsurface treatment, the SPT counts for the improved zone were 2 to 3 times greater.

Table 2.1 Use of Polyurethane in Different Industries (American Chemistry Council 2013)

Application	**Usage (millions of pounds)**	**Percentage of total**
Building & Construction	1,459	26.8%
Transportation	1,298	23.9%
Furniture & Bedding	1,127	20.6%
Appliances	278	5.1%
Packaging	251	4.6%
Textiles, Fibers & Apparel	181	3.3%
Machinery & Foundry	178	3.3%
Electronics	75	1.4%
Footwear	39	0.7%
Other uses	558	10.2%
Total	5,444	100%

2.2 Recent Studies on Mechanical Behavior of Ballast Layer

2.2.1. Ebrahimi et al. (2011)

A large-scale, cyclic triaxial equipment and testing protocol were developed to measure plastic deformation of fouled railway ballast. Different type of fouling, fouling index, moisture, and state of stress were applied in the ballast. FI was calculated by summing percent particles passing 4.75 mm (P4) and percent particles passing 0.075 mm (P200). When the FI is above 20%, ballast was considered to be highly fouled. Large-scale cyclic triaxial was conducted and 200,000 loading repetitions were applied. The results indicated that the plastic strain, ε_p, of the clean ballast was 0.75%. However, the ballast with 20% FI, plastic strain was found as 6.9%. This clearly shows that the amount of fouling content increases the plastic strain of the ballast layer. The ballast fouled with 20% FI was tested with different water contents (3%, 8%, 10% and 14%). According to test results the amount of water content increases the plastic strain of the ballast layer.

2.2.2 Keene et al. (2012)

Keene et al. (2012) studied the mitigating ballast fouling impact and enhancing rail freight capacity. The rigid polyurethane foam (RPF) was injected in to the clean ballast. Polyurethane stabilized ballast (PSB) specimens were prepared by refining the polyurethane in jection methodology. The cyclic triaxial tests were conducted stabilized specimens at a deviator stress of 300 kPa. PSB deformational behavior varied as RPF density varied. The PSB specimen with no confinement had cumulative plastic stain, ε_P, of 0.43% or 63% less than clean ballast over 200,000 loading cycles. The PSB specimens with full confinement of 90 kPa had cumulative ε_P of 0.15%, i.e., 87% less than the clean ballast. Monotonic-flexural loading was also conducted on beam specimens to measure the rupture strength. From the flexural tests conducted, the flexural strength increased as the percent RPF by weight of the specimen

increased. According to flexural fatigue test results the average rupture strength was 938 kPa with a coefficient of variation (COV) of 23.7%. Unconfined compression was conducted to measure the PSB strength and Young's modulus. The average strength of the PSB prisms (half of the beam specimen) was 2.60 MPa. The average Young's modulus determined from the unconfined compression strength (UCS) tests was 89.7 MPa. This study also compared the failure mode of PSB to concrete showing that concrete yields around 0.002 m/m, whereas PSB yields around 0.02 m/m (i.e., an order of magnitude greater); however, the minimal yield strength of concrete is designed around 21 MPa (3,000 psi) and the PSB yielded around 1.5 MPa (220 psi), 90% less. Based on these attributes, the compliance (i.e., yield strain) of PSB is much more than concrete.

2.2.3 Dersch et al. (2010) and Boler (2012)

Dersch et al. (2010) and Boler (2012) used rigid-compact polyurethane to coat the ballast particles. The direct-shear box test was conducted under varying normal stresses to measure shear strength of the reinforced ballast. Depending on the test results, the shear strength of coated ballast specimen was 40-60% greater than uncoated clean ballast. After direct share test, a powdering test was conducted and results showed that coated ballast samples had 3-5% less breakage than untreated ballast. As a result, polyurethane treatment greatly increases shear strength of ballast and reduces fouling due to the breakage of ballast particles under loading.

2.2.4 Kennedy et al. (2009)

Kennedy et al. (2009) conducted full-scale model tests to determine the deformational characteristics of the ballast layer with and without polyurethane. Rigid-compact polyurethane, which is similar to the type used in the study by Dersch et al. (2010), was injected on and into the ballast layer. In their study, 500,000 loading repetitions which simulate railway traffic loading conditions was applied to full-scale model to measure plastic strain of ballast. The results

showed the settlement of the ballast layer in the model was 95-98% less for the treated full-scale model substructure than the untreated substructure modeled at their facility.

3. MATERIALS AND METHODS

3.1 DOLOMITIC BALLAST

The dolomitic ballast (Fig. 3.1) used in this project was provided by the BNSF Railway Company. This dolomitic ballast has similar characteristics to the granitic ballast used in Keene et al. (2012) and Ebrahimi et al. (2011) and conforms to the AREMA No. 24 gradation (Fig. 3.2), with particle sizes between 26 mm and 76 mm, the coefficient of uniformity, C_u, of 1.78, and coefficient of curvature, C_c, of 1.32. The dolomitic ballast was a sub-angular to angular, poorly graded, coarse gravel. Maximum ballast dry density was determined using the procedure from Ebrahimi et al. (2011), which resulted in a void ratio, e_b, of 0.60 and a slightly lower dry unit weight, γ_d, of 15.6 kN/m^3 due to the lower specific gravity, SG, of 2.58 of the dolomitic rock.

Figure 3.1 Picture of Dolomitic Ballast Used in the Study

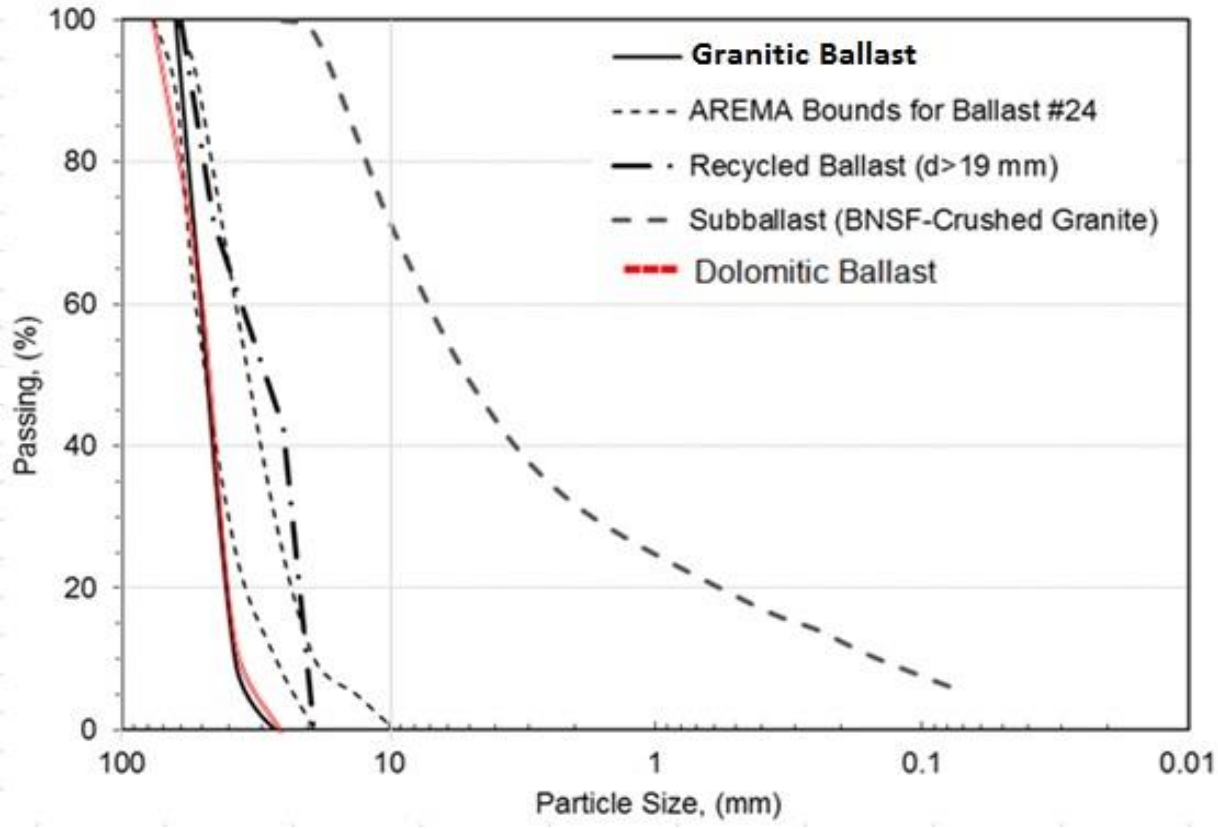

Figure 3.2 Gradations of Ballast Types Used in This Study

3.2 GRANITIC BALLAST

To determine if ballast type contributes to PSB behavior, a several specimens were comprised of the granitic ballast (Fig. 3.3) from Keene et al. (2012), which was the same granitic ballast characterized by Ebrahimi et al. (2011), where the particle-size distribution (ASTM D6913) showed particle sizes of 25–63 mm and conformed to the AREMA No. 24 ballast gradation specification (Fig. 3.4). Maximum dry density was verified using the procedure developed in Ebrahimi et al. (2011), resulting e_b of 0.62. Corresponding clean ballast dry unit weight (γ_d) and density (ρ_d) were 15.8 kN/m^3 and 1,611 kg/m^3, respectively. The specific gravity of the granitic ballast was 2.6. These compaction characteristics were targeted for fabrication of each specimen of clean ballast in this study.

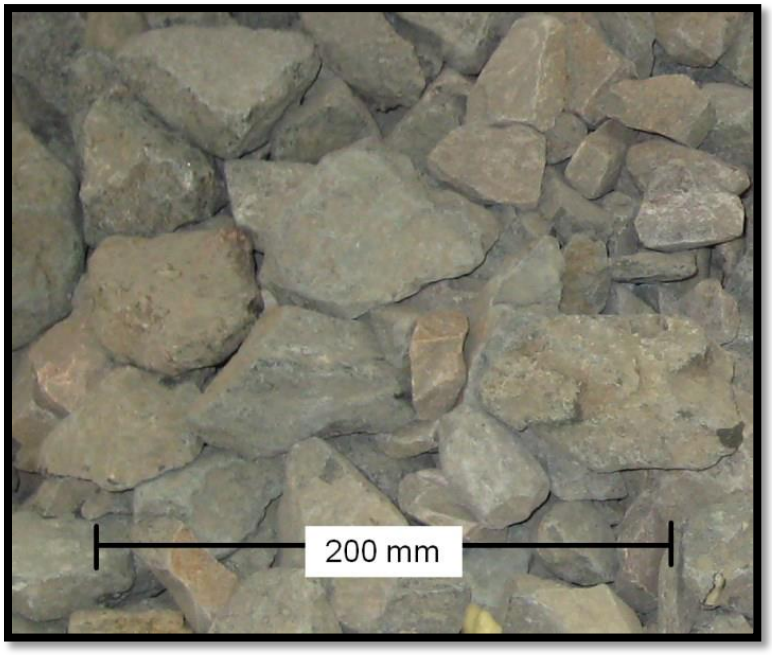

Figure 3.3 Picture of Granitic Ballast Provided by the BNSF Railway Company from a Quarry Near Cheyenne, Wyoming (Keene at al., 2012).

3.3 Fouled Ballast

The fouled ballast was prepared by mixing clean ballast with fouling material (described below) and water in the same manner as outlined in Keene et al. (2012). The FI and water content (WC) were defined based on the designation from Selig and Waters (1994) as shown in Table 3.1. The FI consists of summing the percentage of particles passing through a 4.75-mm (P4) sieve with the percentage of particles passing a 0.075-mm (P200) sieve. The ballast was prepared consistent with 80% P4 and 20% P200, which is similer to the fouled ballast meterial based on Wisconsin & Southern Railroad, L.L.C. (WSOR) tested by Ebrahimi et al. 2011)

3.4 Fouling Materials

Clay

The clay fouling material used in this project was a Kaolinite from Columbus Clay Co. located in Columbus, Ohio (see Fig. 3.6a). The specific clay used was Kaolin (EPK). Using ASTM D 4318 the liquid limit (LL) was 52% and the plasticity index (PI) was 25.

Coal

The same coal material used in Ebrahimi et al. (2011) was also used in this study (see Fig. 3.6b). Coal fouling was obtained by grinding Wyoming-based coal to produce particles with a size distribution similar to typical coal fouling that has been observed in the field (Huang et al. 2009). Coal fouling has low plasticity and is collectively referred as non-cohesive fouling material (Table 3.1).

Frac Sand

Because of recent increases in transporting frac sand by rail, fouling from frac sand is a potential problem in Wisconsin and elsewhere (Hesse, 2014). Thus, frac sand (see Fig. 3.6e) was used in two samples in this study as a fouling material. The frac sand was 20/40 Quartz sand. The 20/40

determines that 50% was retained on a #20 sieve, and the remaining 50% on the #40 sieve. This sand was obtained from quarry in Ottowa, IL (Hesse 2014) provides a through review of this sand type and characteristics.

Granitic Fouling

Granitic fouling (see Figure 3.6d) was obtained by fractioning highly fouled ballast obtained from WOS Railroad Company. The fraction passing a No. 4 sieve (4.75 mm), based on the criteria by Selig and Waters (1994), is designated mineral fouling (Figure 3.4). This was the same fouling type and gradation used in Ebrahimi et al. (2011).

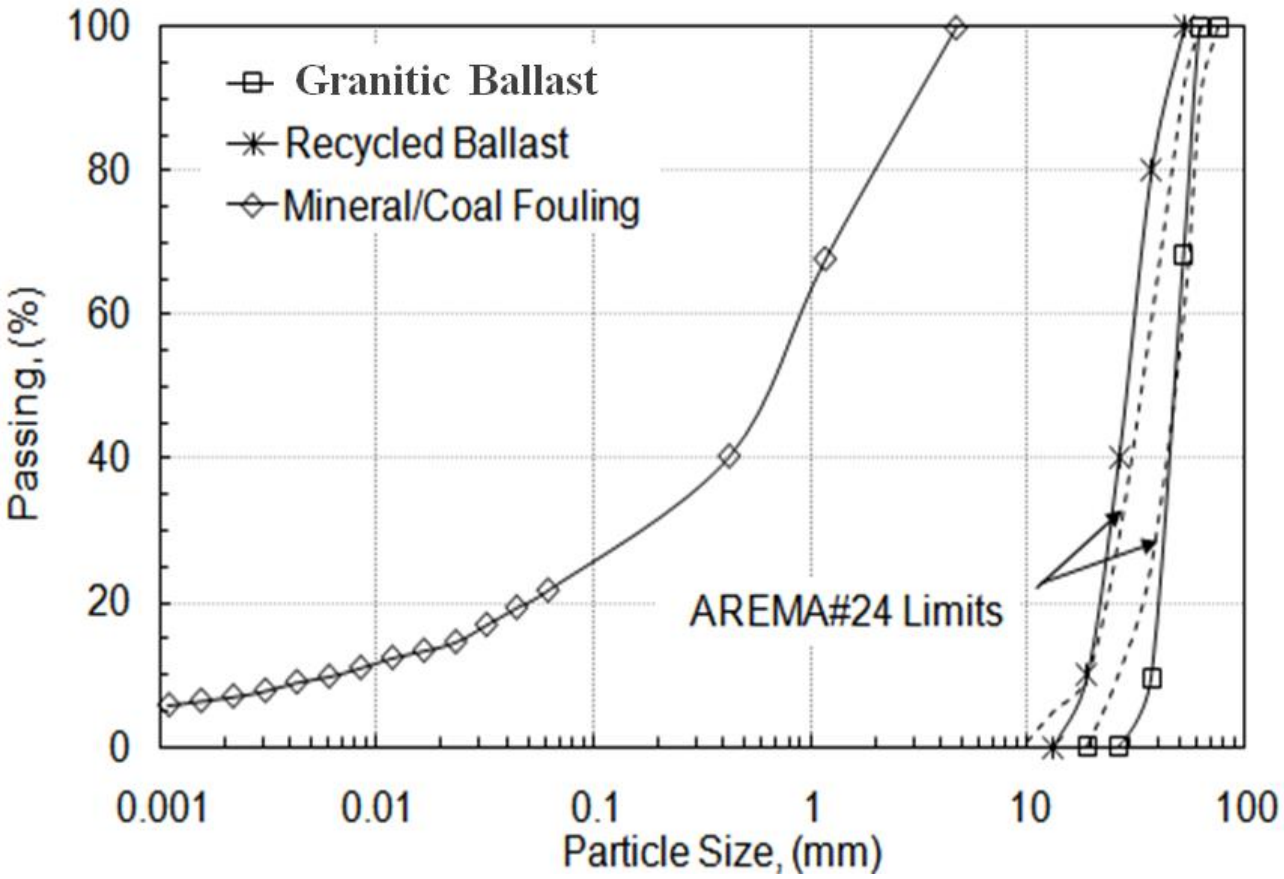

Figure 3.4 Gradations of Non-Cohesive Fouling Material Selig and Waters (1994)

Table 3.1 Index Properties of Ballast and Non-Cohesive Fouling Materials Ebrahimi et al. (2011).

Sample	D_{50} (mm)	C_u	C_c	G_s	LL (%)	PL (%)	e_B	Sand Content (%)	Fines Content (%)	USCS Symbol
Granitic Ballast	53	1.4	0.6	2.6	NA	NA	0.62	0	0	-
Mineral Fouling	1	113	4.5	2.6	20	NP	-	100	20	SM
Coal Fouling	1	113	4.5	1.3	31	NP	-	100	20	SM
Dolomitic Fouling	24	43	0.8	2.5	NA	NA	0.66	0	0	-

Note. NP = not plastic, NA = not applicable, D_{50} = median particle size, C_u = coefficient of uniformity, C_c = coefficient of curvature, G_s = specific gravity, LL = liquid limit, PL = plastic limit, e_B = void ratio of ballast. Particle size analysis conducted following ASTM D 422, G_s by ASTM D 854, USCS classification by ASTM D 2487, and Atterberg limits by ASTM D 4318.

Dolomitic Fouling

The dolomitic fouling was obtained from Wingra Stone Co. in Fitchburg, WI (see Fig. 3.4c). The fouling material was the result of crushing dolomitic/limestone rocks from aggregate base courses used in roadway construction. Figure 3.5 shows the dolomitic fouling material grain size distribution. This dolomitic fouling material was used in conjunction with the dolomitic ballast to keep mineralogy similar.

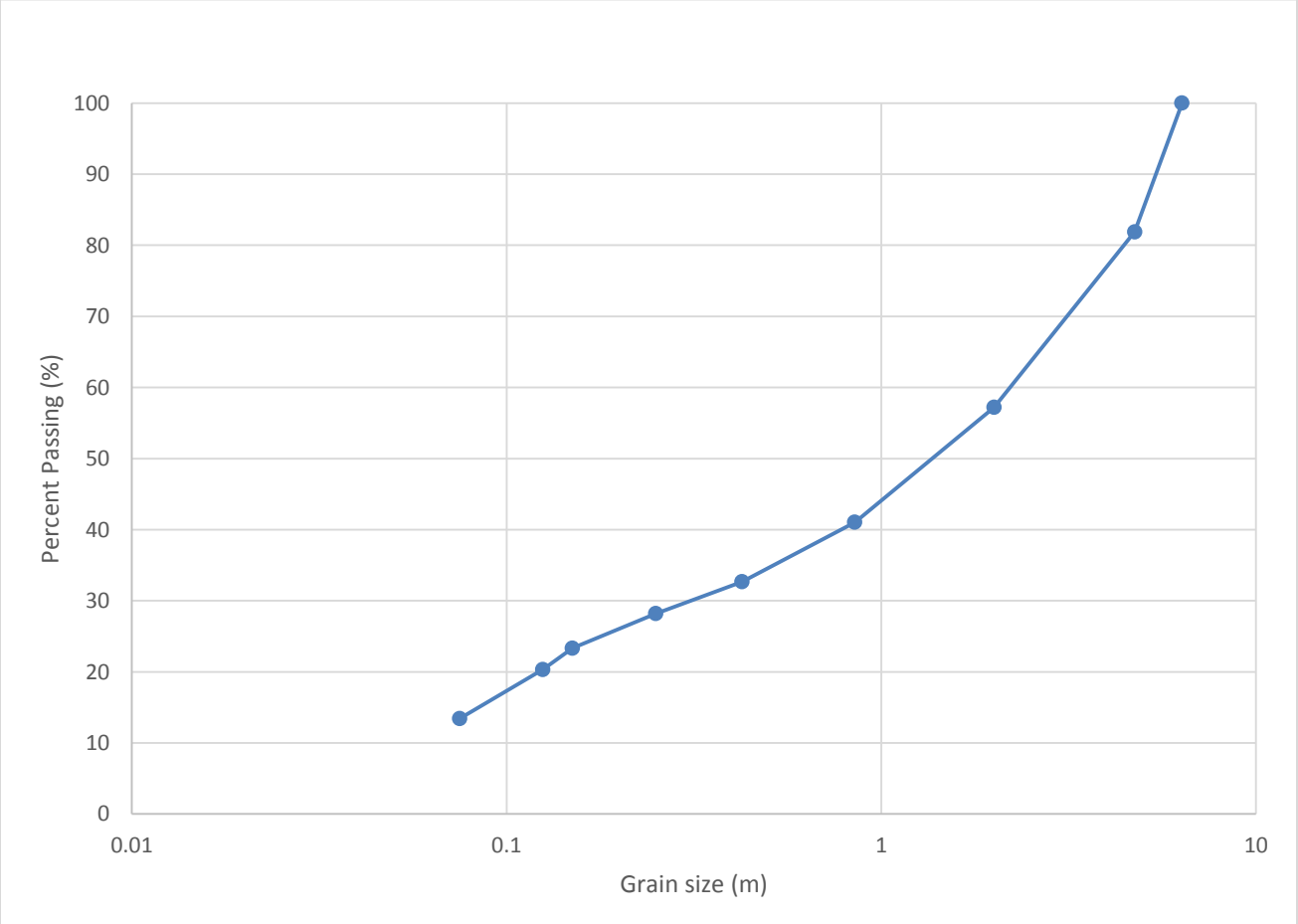

Figure 3.5 Gradations of Non-Cohesive Dolomitic Fouling Material

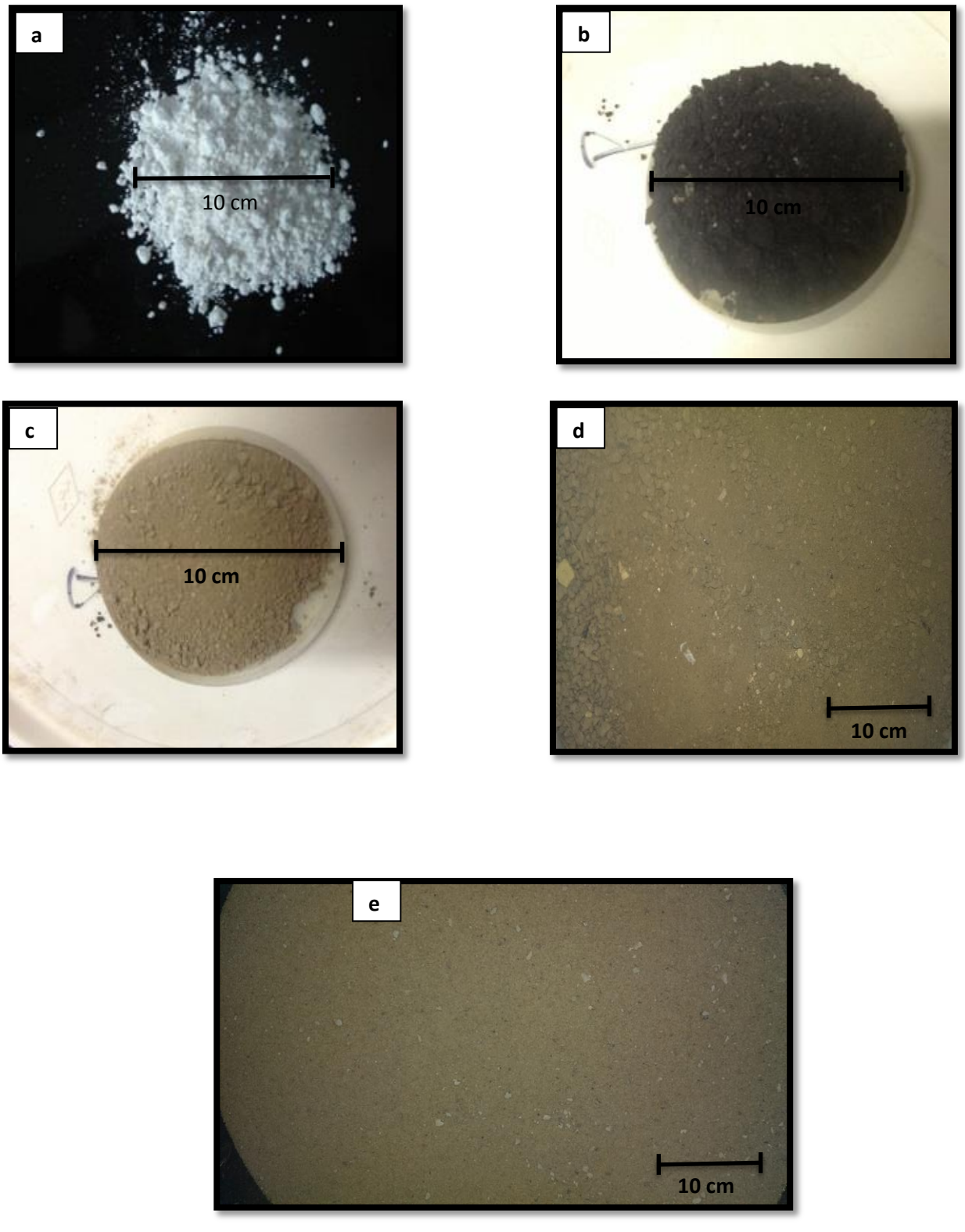

Figure 3.6 Pictures of Different Fouling Materials: (a) Clay, (b) Coal, (c) Dolomitic Mineral Fouling, (d) Granitic Mineral Fouling, and (e) Frac Sand

3.5 Rigid-Polyurethane Foam (RPF) - (486STAR-4 BD)

Rigid-polyurethane foam (RPF) – (486STAR-4 BD) is a two-component, high-density, expanding, thermoset, polyurethane-resin system. The RPF was formulated by Bayer Material Science for different applications including void filling and sealing. The RPF (Fig. 3.7a) occurs by mixing two primary chemical components, which are polyester or polyether polyol and organic polyisocyanate proportionately in the presence of a catalyst. The cellular structure of the RPF is a closed-cell structure as defined by Szycher (1999). The specific elastomer system was developed in partnership with Uretek USA Inc. Uretek USA Inc. supplied the material and assisted in specimen fabrication.

3.6. Polyurethane Stabilized Fouled Ballast (PSFB)

RPF is used to fill the void spaces in the fouled ballast which is the clean ballast mixed with different fouling materials corresponding to different (FI) and water content (WC) in the same manner as outlined in Keene et al. (2012). RPF was injected to in the fouled ballast, the polyurethane could expand and flow thorough the pore space. RPF provides bounding between particles while RPF is transitioning from the gel phase to the concrete phase (Keene et al. 2012). In this transition RPF establishes bonds with materials. The bonding properties are unique due to the interaction of the polyurethane with the aggregates. A fouled ballast sample stabilized with RPF is called polyurethane stabilized fouled ballast (PSFB) in this study (Fig. 3.7b)

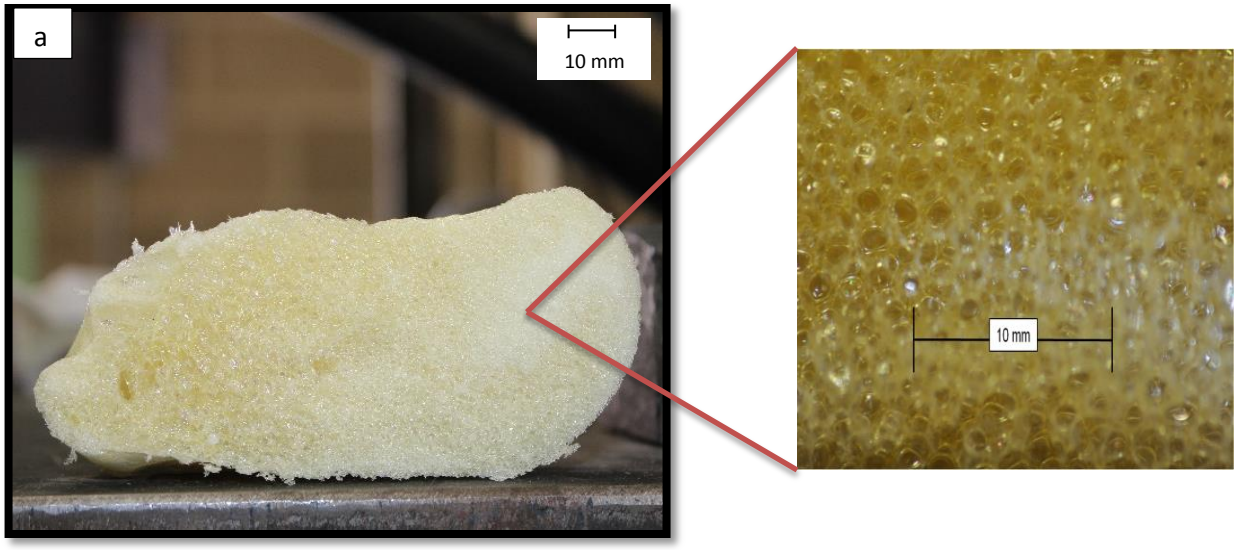

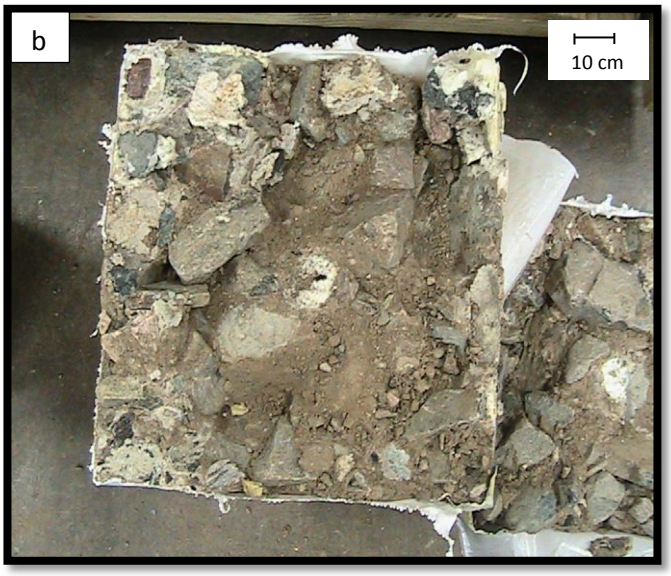

Figure 3.7 Picture of (a) RPF and (b) PSFB Created During the Study

3.7. POLYURETHANE STABILIZED BALLAST (PSB)

To provide a reference in assessing the effectiveness of polyurethane stabilization of fouled ballast, a clean dolomitic ballast (FI = 0%, WC = 0%), was fabricated and stabilized with RPF. This specimen is called polyurethane stabilized ballast (PSB) in this study (Fig. 3.8)

Figure 3.8 Picture of Polyurethane Stabilized Ballast (PSB)

3.8 SPECIMEN PREPARATION

3.8.1 Cylindrical Specimens

The specimen fabrication molds were designed to create (PSFB) specimens that could be tested for mechanical properties using the protocols laid out in previous research. The objective was to create cylindrical specimens for cyclic triaxial compression testing. A cylindrical mold (Fig. 3.9a) was made from hard cardboard tube (quick-tube). Dimensions for the cylindrical samples used for the cyclic triaxial testing had a diameter of 254 mm and maintained an appropriate ratio of ballast particle diameter to specimen diameter. In this study the cylindrical molds dimension were increased by 1:6 ratios because of the ballast particle size which is granular material. These dimensions were reasonable base on a study by Anderson and Fair (2008) on triaxial testing of railway ballast. Keene et al 2012 assumed that five or six ballast particles should be fit in diameter of 254 mm. Although the 254 mm diameter sample does not fulfill the ASTM D 5311 guideline of 1:6 ratio, by Keene et al. (2012) noted that the ratio of does not impact results.

The mold was covered inside with plastic sheeting to prevent the mold surface from contacting polyurethane. To prepare a fouled ballast specimen, the ballast and fouling materials were mixed to yield different fouling indices and water content and the ballast particles are coated by fouling materials. The fouled ballast was placed in five layers in the mold and each layer was compacted with hammer. A 100-N hammer with a base area of 72 cm^2 was dropped at a height of 100 mm for 40 – 45 repetitions for each compaction lift. Fouled ballast specimen was drilled along the specimen length at the center of the specimen to place an injection rod. Table 3.2 shows the amount of FI and WC of 19 cylindrical PSFB specimens that were used in this study (See Fig. 3.9b).

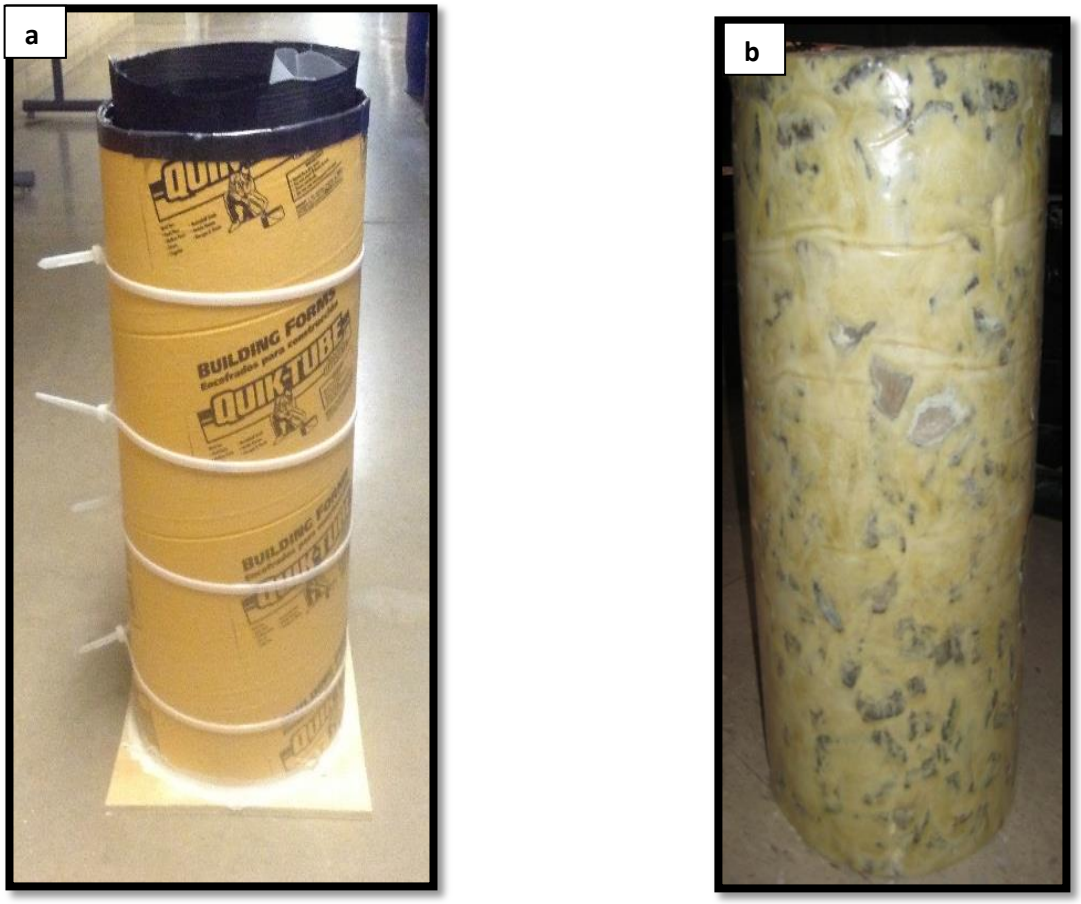

Figure 3.9 Cylindrical Mold (a), Cylindrical PSB (b) after Injection

Table 3.2 Cylindrical Specimen FI and WC Distribution

Sample	FI %	WC %	Ballast Type	Fouling Type
1	10	6	Dolomite	Dolomitic Mineral Fouling
2	10	20	Dolomite	Dolomitic Mineral Fouling
3	15	6	Dolomite	Dolomitic Mineral Fouling
4	15	20	Dolomite	Dolomitic Mineral Fouling
5	20	6	Dolomite	Dolomitic Mineral Fouling
6	20	20	Dolomite	Dolomitic Mineral Fouling
7	0	0	Dolomite	No fouling
8	24	14	Dolomite	Frac Sand
9	10	14	Dolomite	Clay Fouling
10	10	14	Dolomite	Clay Fouling
11	20	24	Dolomite	Clay Fouling
12	20	24	Dolomite	Clay Fouling
13	12	8	Dolomite	Coal Fouling
14	12	14	Dolomite	Coal Fouling
15	24	8	Dolomite	Coal Fouling
16	24	14	Dolomite	Coal Fouling
17	24	14	Granite	Frac Sand
18	20	17	Granite	Clay Fouling
19	15	13	Granite	Granitic Mineral Fouling

3.8.2 Beam Specimens

Beam specimens for flexural testing and half-beam specimens for unconfined compression strength (UCS) testing were also created. A beam mold (see Fig. 3.10a) was made from wood and the inside was covered with plastic sheeting to seal the mold and to prevent the mold surface from contacting the polyurethane such that the specimen could be removed easily. Dimensions for typical cement-stabilized soil beams used for flexural and unconfined compression testing are provided in ASTM D1635, 76 mm x 76 mm x 290 mm. For this study the dimensions of the beams were increased by a ratio of 2.63:1 to account for the large particle sizes of ballast. The dimensions used for the PSFB beam molds were therefore 200 mm x 200 mm x 763 mm. Although, this is smaller than the 1:6 particle size to diameter ratio, optimum ballast density of 15.6 kN/m^3 was still achieved. To prepare a fouled ballast specimen, the ballast was mixed with moist fouling material to the target fouling indices as presented in Table 3.3. The fouled ballast was placed in five layers in the beam mold and each layer was compacted with a 100-N hammer at a height of 100 mm for 40 – 45 repetitions. Figure 3.10b shows a PSFB beam specimen used in this study.

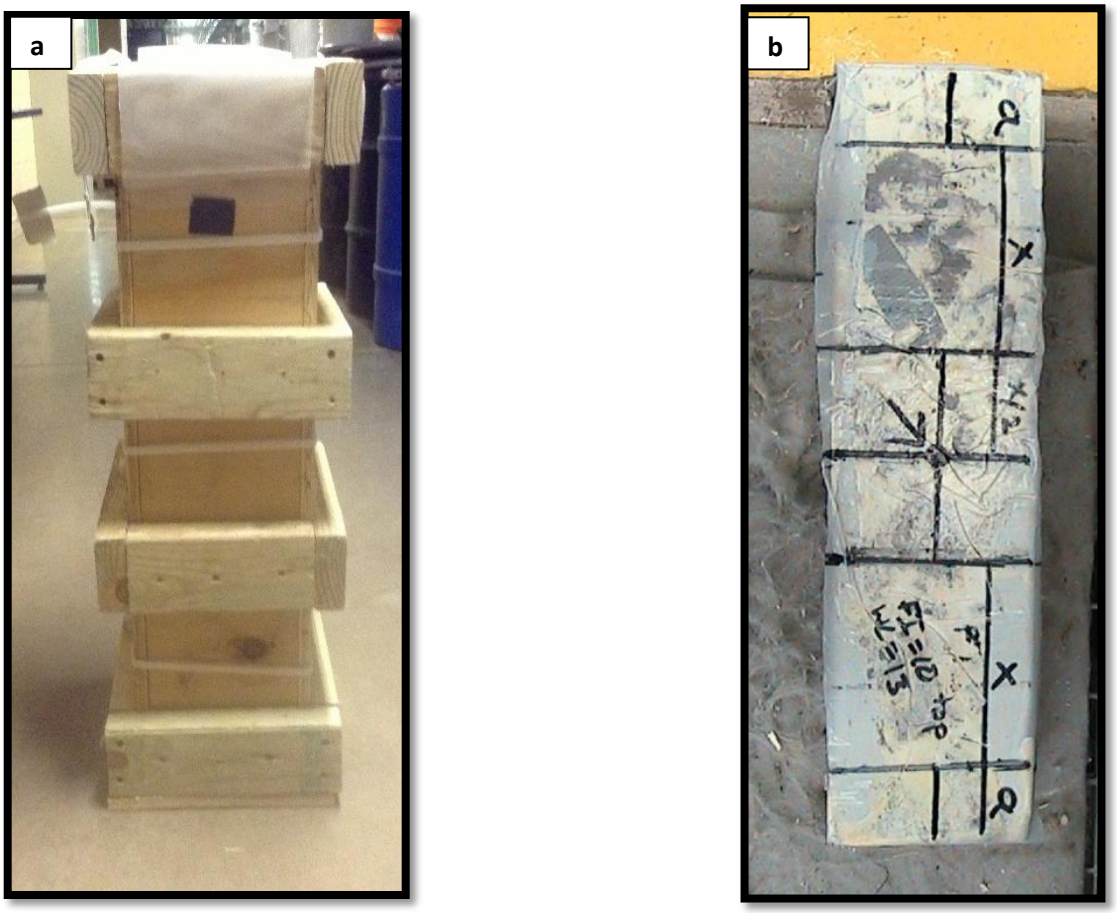

Figure 3.10 Picture of Beam Mold (a); Beam PSFB (b) after Injection

Table 3.3 Beam Specimen FI and WC Distribution

Sample	FI %	WC %	Ballast Type	Fouling Type
1	15	13	Dolomite	Dolomitic Mineral Fouling
2	15	8	Dolomite	Dolomitic Mineral Fouling
3	10	13	Dolomite	Dolomitic Mineral Fouling
4	10	8	Dolomite	Dolomitic Mineral Fouling
5	0	0	Dolomite	Dolomitic Mineral Fouling

3.9 PHASE RELATIONSHIPS

To order to determine the proper amount of polyurethane to inject, phase relationships were calculated for each specimen. Besides the control specimen, used to verify Keene et al. (2012) results, every specimen was made of four phases: air, water, fouling material, and ballast. Following the second approach of sample preparation in Keene et al. (2012), the goal of the injections was to inject a quantity that would not affect geometry by foam expansion. Using an injection method like this would be advantageous for modeling mechanical behavior that could be representative of a field application. With the specified weight and initial volume of the compacted ballast, the void ratio and dry density were calculated using a specific gravity of ballast solids of 2.6 for the granitic ballast as determined in Ebrahimi et al. (2011) and 2.58 for dolomitic ballast. After RPF injection, each PSFB specimen was weighed (WPSB) and measurements taken to determine the final volume (VPSB). The PSFB density (ρ_{PSFB}) was determined by

$$\rho_{PSFB} = \frac{W_{PSFB}}{V_{PSFB}} \qquad \text{Eq. (3.1)}$$

A phase diagram (Fig. 3.11) illustrates the phase relationships (i.e., densities of ballast and RPF) within the PSB composite.

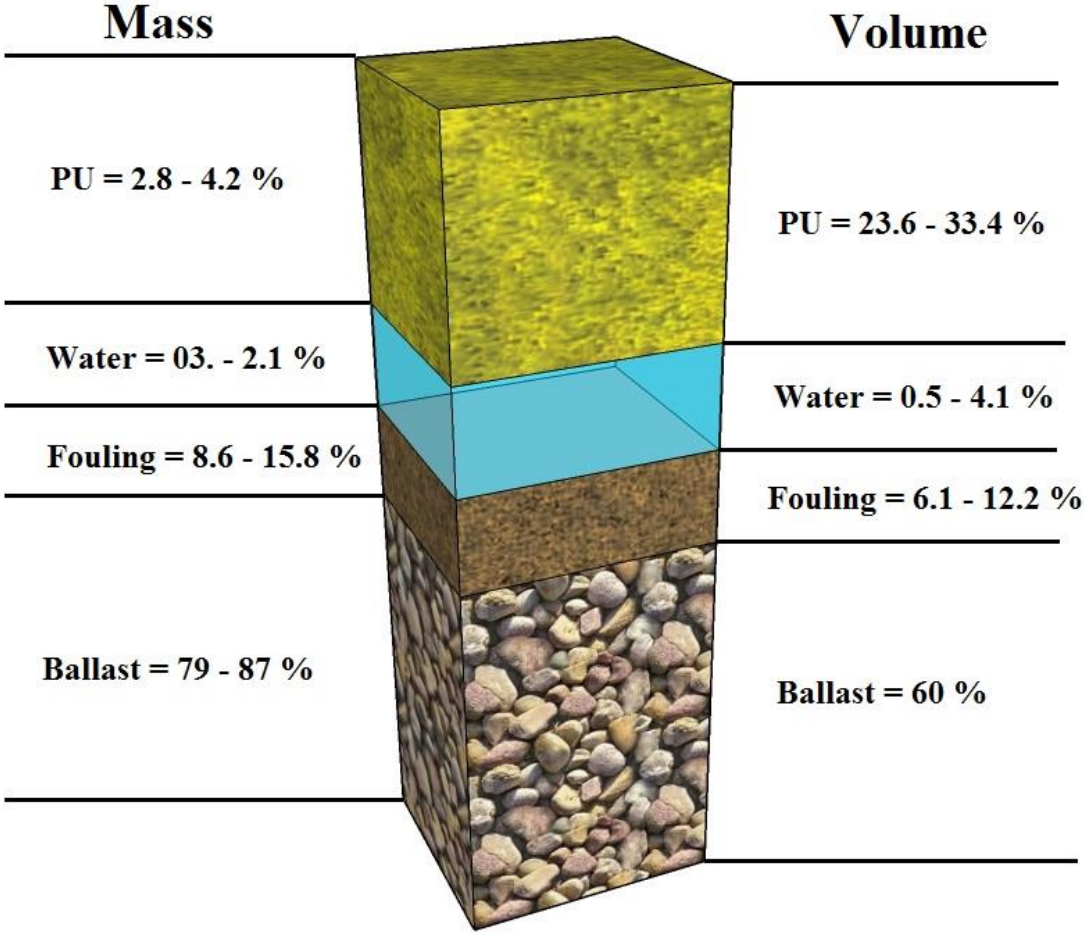

Figure 3.11 Example Phase Relationships

3.10 POLYURETHANE INJECTION

Based on the phase diagram after compaction, the void space was calculated. This void space would be theoretically filled with polyurethane after the injection. The injection times for this study were significantly lower than Keene et al. (2012) due to fouling. Total injection time was between 38-50 s, but with only 13 – 25 s of that time, the polyurethane being actively injected. Prior to sample injection, the polyurethane's reaction curve was measured and if satisfactory reaction times were achieved the fabrication would continue (Fig.3.12).

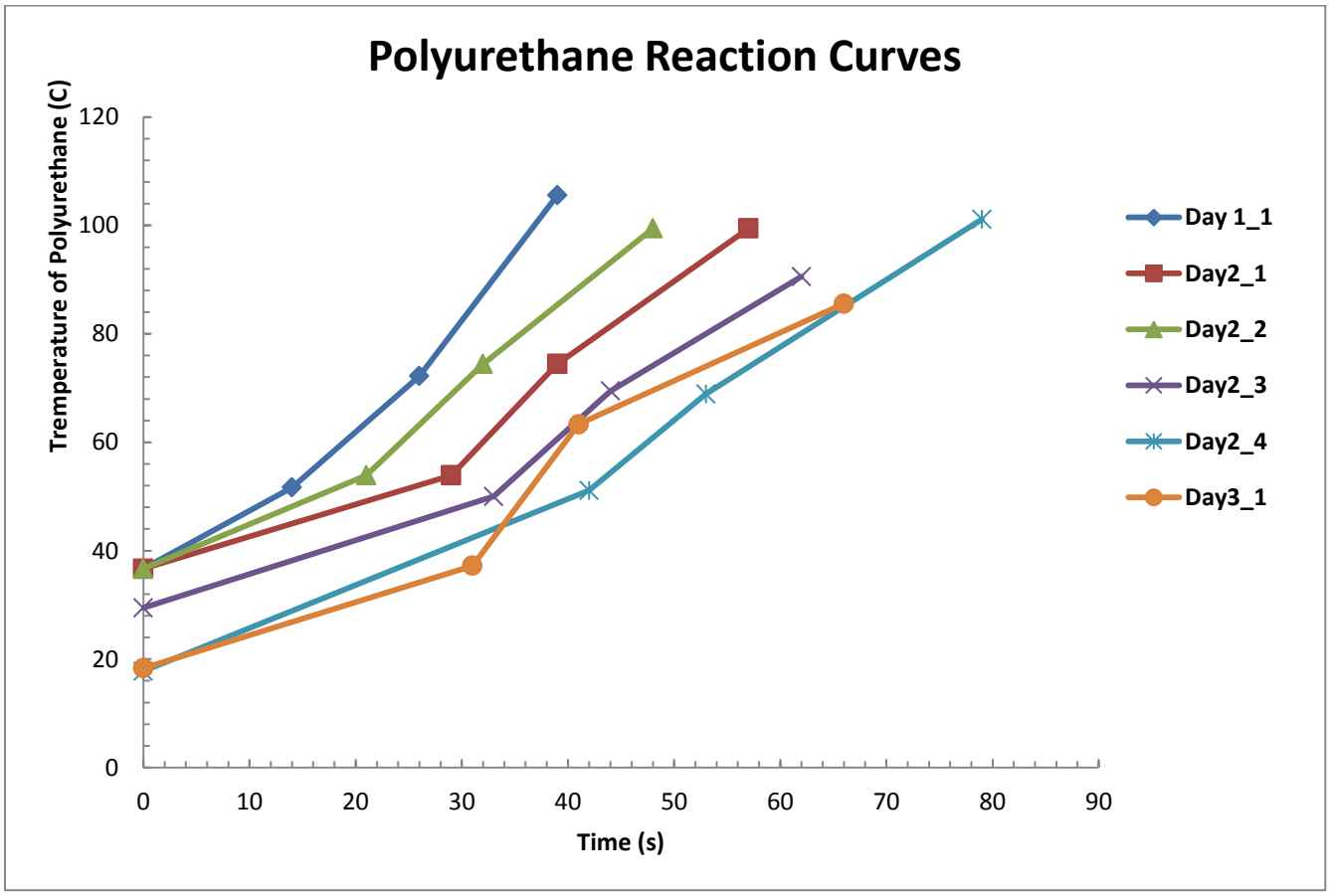

Figure 3.12 Polyurethane Reaction Curves

In Fig.3.12 the initial temperatures are on the left hand side of each day's respective curve. Due to limits of the available measurement equipment, the final phase in the polyurethane reaction, End-of-Rise, could not be established; therefore, it was omitted. The four points on the graph show the start, cream, gel, and tack free phases of six reaction curves shot direct unconfined injection of polyurethane on a plane surface. The elbows of Day 2_1 and Day 3_1 curves are attributed to cold outside temperatures (3 °C), and the equipment not operating at the correct temperature (30 °C).

Once the reaction curve was deemed acceptable, a time vs. weight calibration was done on the injection equipment. This was how the desired amount of polyurethane was calculated using the phase diagrams. The cylindrical specimens with dimensions D 254 mm x H 508 mm would have a specified injection quantity at the base, at 154 mm from the base, at 305 mm from the base, 457 mm from the base, and at the top. The beam samples, with dimensions 200 mm x 200 mm x 763 mm, would have a specified injection quantity at the base, 152 mm from the base, 304 mm from the base, 457 mm from the base, 611 mm from the base, and at the top. After the injections took place, the specimens were allowed to cure for 24 h, the mold was removed, and the specimens were sealed to keep moisture constant.

4. MECHANICAL PROPERTY TESTING METHODS

4.1 MONOTONIC FLEXURAL TESTING OF BEAMS

4.1.1 Methodology

Monotonic-flexural loading test is used for determining flexural strength of bound materials that undergo bending stresses in transportation infrastructure, such as concrete, asphalt, and cement-stabilized soils. For testing of PSB and/or polyurethane-stabilized fouled ballast (PSFB), beam specimens were chosen to determine the flexural strength. In pavement layer design, flexural strength of materials is an important factor for determining slab thickness. In the case of polyurethane-stabilized materials, the flexural strength may be an important factor if stabilization creates layers that begin to act as in situ continuous slabs, which would be below the subsurface where visual signs of degradation tend to go unnoticed. A "third-point" loading setup is ideal for reducing the effects of shear stress during flexural testing and allows realistic analysis of flexural strength. Dimensions for typical cement-stabilized soil beams are provided in ASTM D1635 and Midgley and Yeo (2008). These dimensions were 76 mm x 76 mm x 290 mm; in this study, the dimensions of the beams were increased by a ratio of 2.63:1 to account for the large particle size of ballast. The dimensions used for the PSFB and PSB beam molds were 200 mm x 200 mm x 763 mm.

4.1.2 Analysis of Monotonic Flexural Tests

The flexural strength of the beams was determined using protocols from ASTM C78 and ASTM D1635. In the standards, constant rate of loading is applied until the beam specimen ruptures. The load is applied to a fixture that distributes the load evenly through two loading rollers at the two center "third-points" of the beam and the beam is supported by rollers on the two outer "third-points" of the beam. The flexural strength (R), is calculated by;

$$R = \frac{PL}{wh^3} \qquad \text{Eq. (4.1)}$$

where P is the peak load (kN) during the test or load before rupture, L is the span length (m), w is the base width (m) of the beam, and h is the depth (m). Figure 4.1 shows the 3D monotonic flexural test equipment and dimensions.

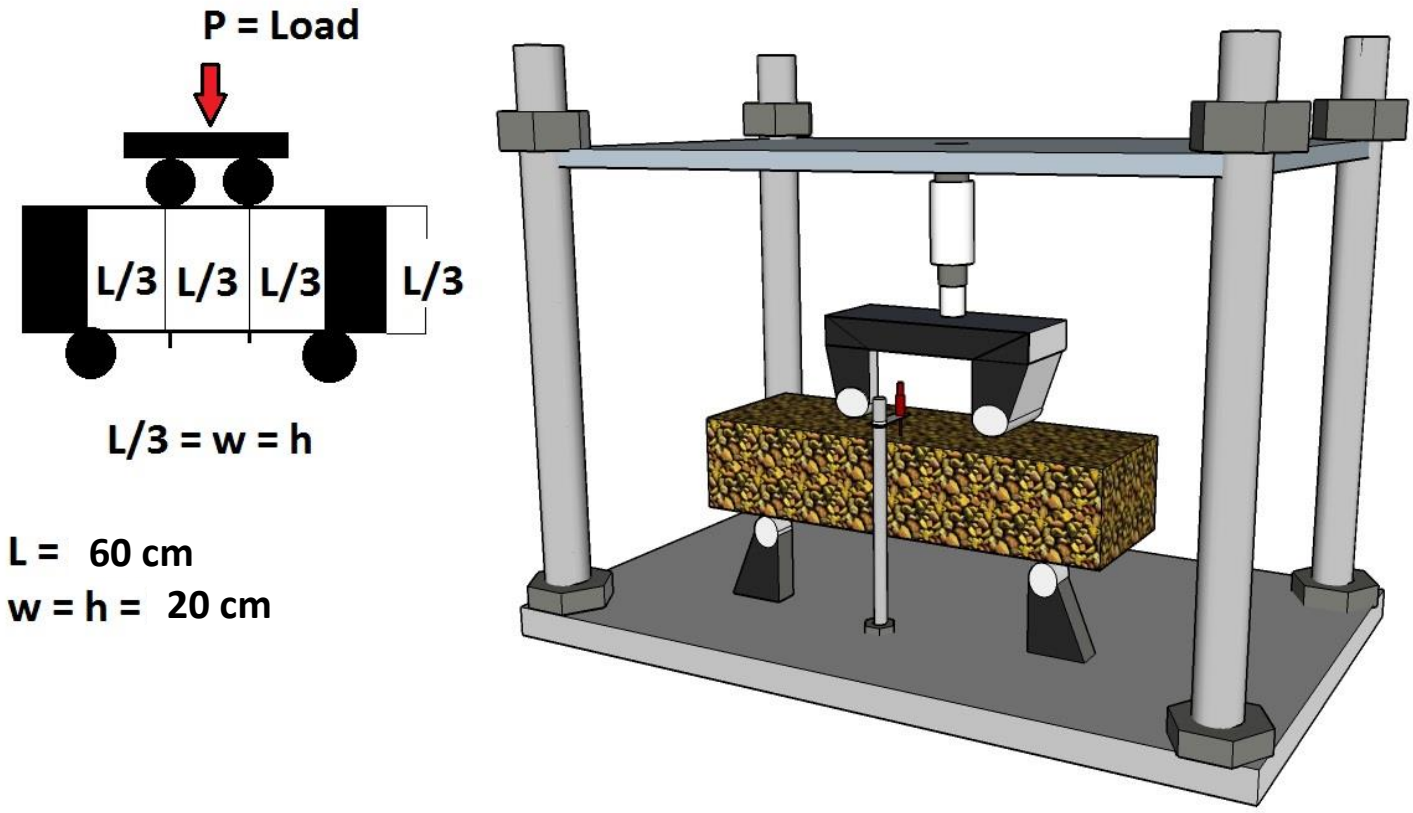

Figure 4.1 Third-Point Loading Setup and Chosen Dimensions for PSFB and PSB Beam Samples.

4.2 UNCONFINED COMPRESSIVE STRENGTH TESTING

4.2.1 Methodology

Unconfined compressive strength (UCS) testing (see Figure 4.2) is typically used for determining strength and elastic modulus of materials as a reference index to verify that other mechanical properties can be confirmed in the material. The strength and modulus of the PSFB prisms were found to correlate with the phase properties (i.e., PSFB density, ballast density, percent RPF by weight, etc.) of the specimens, After rupture of PSFB and PSB beams, remaining segments of the beams were cut with a concrete masonry saw to a 2:1 height-to-width ratio (PSFB prisms) and subjected to unconfined compressive strength (UCS) tests. A 2:1 height to width ratio was selected to reduce the effect of friction at the ends of the specimens (Bishop and Green 1965). This minimal height-to-width ratio is also recommended in applicable unconfined compressive strength test standards, which included ASTM D7012 for compressive strength and elastic moduli of intact rock core specimens and ASTM D1621 for compressive properties of rigid cellular plastics. Methodology from each of these standards was combined for testing on PSFB and PSFB prisms and subsequent analysis. Load was applied to the prisms through a servo-hydraulic system (SATEC®, loading capacity of ~1,780 kN). Vertical deflection of the specimens was measured using extensometers as part of the SATEC NuVision Computer system during monotonic loading. The stress rate recommended in ASTM D7012 is 0.5 to 1.0 MPa/s for intact rock core specimens. The nominal stress rate used in PSFB prism testing was 0.834 MPa/s.

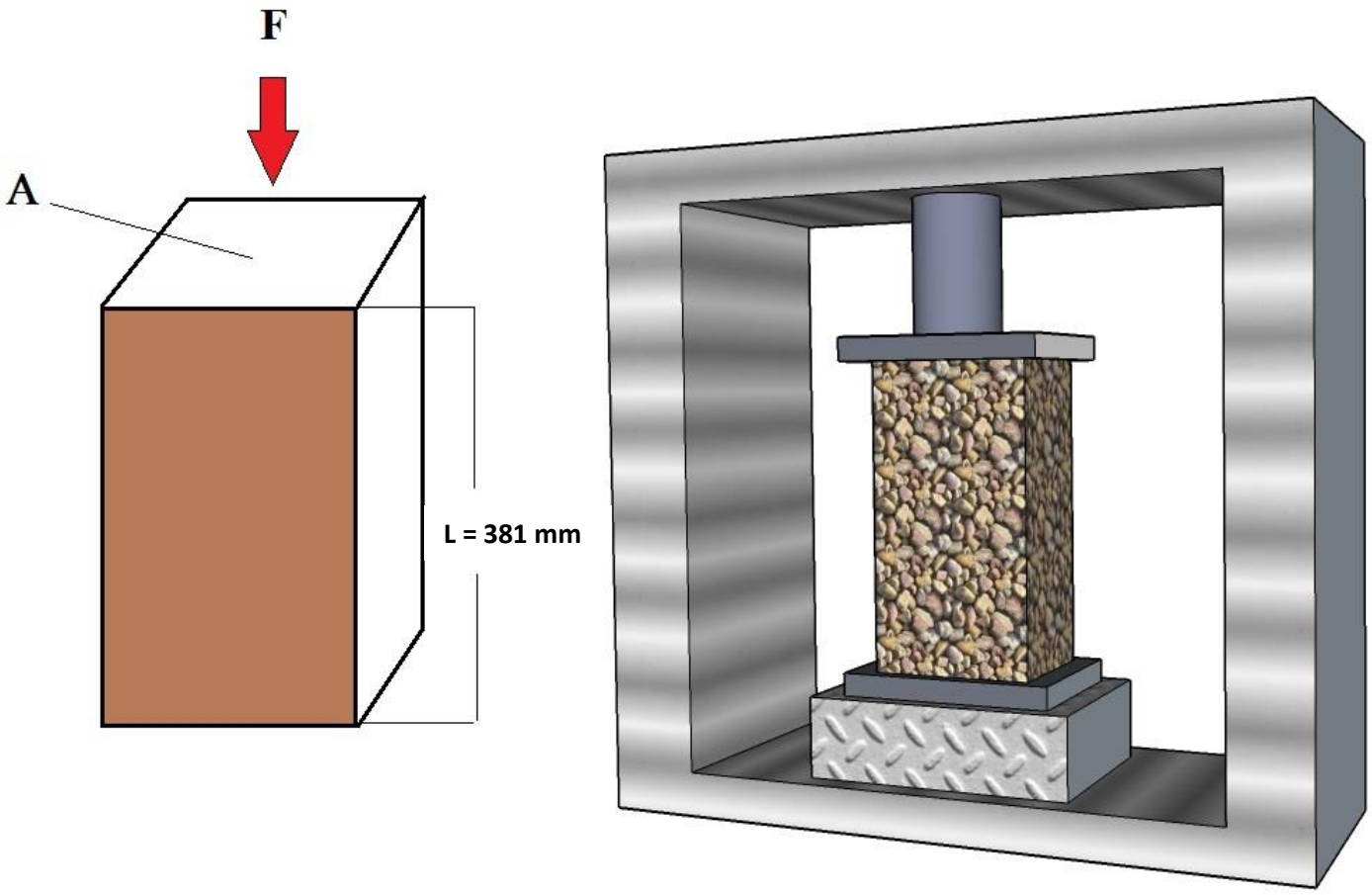

Figure 4.2 UCS Testing Apparatus and Diagram of Compression Testing Parameters.

4.2.2 Analysis of Unconfined-Compression Tests

Unconfined compressive strength (σ_c) is

$$\sigma_c = \frac{F}{A} \quad \text{Eq. (4.2)}$$

where F is peak axial load applied and A is the area over which it is applied. A typical phenomenon in elastic-plastic material is that initially elastic strain (ε_e) increases linearly with axial stress until reaching the yield point, where plastic strain (ε_e) increases and the relationship to stress is no longer linear. Elastic modulus, E, occurs within the linear region and is defined by

$$E = \frac{\sigma_a}{\varepsilon_e} \quad \text{Eq. (4.3)}$$

where σ_a is the axial stress being applied within the elastic range of the material.

4.3 CYCLIC TRIAXIAL COMPRESSION TESTING

4.3.1 Methodology

Large scale cyclic triaxial compression test was conducted for determining plastic deformational behavior of cylindrical PSFB samples. Cyclic triaxial testing of ballast and railway materials has been used in several studies (Ebrahimi et al. (2011); Aursudkij et al. 2009; Skoglund 2002; Anderson and Fair 2008). Based on these studies, a cyclic triaxial testing method was chosen for cyclic triaxial compression testing of PSFB and PSB. This type of laboratory test method was chosen to represent rail traffic loading on the substructure that occurs in the field. A

typical triaxial cell used in this study is illustrated in Fig. 4.3. Cylindrical specimens with a minimum diameter (D) of 254 mm maintained an appropriate ratio of ballast particle diameter to specimen diameter; these dimensions were reasonable base on a study by Anderson and Fair (2008) on triaxial testing of railway ballast. The specimens with 304-mm diameter were acceptable based on Skoglund (2002), which presented a minimum ratio (1:6) of particle-size diameter to specimen diameter. A 1:6 ratio is also specified for load controlled cyclic triaxial strength of soil in ASTM D 5311. Load was applied to the cylindrical specimens through a servo-hydraulic system (MTS®, loading capacity of 100 kN). Vertical deflection of the specimens were measured using two (for redundancy) linear variable differential transducers, LVDTs, (Omega, 20 ± 0.05-mm) during cyclic loading. LVDTs were mounted to the loading piston extending into the triaxial chamber through the top plate. Clean ballast specimens were tested in each triaxial cell and the corresponding results were validated with the data found in Ebrahimi et al. (2011).

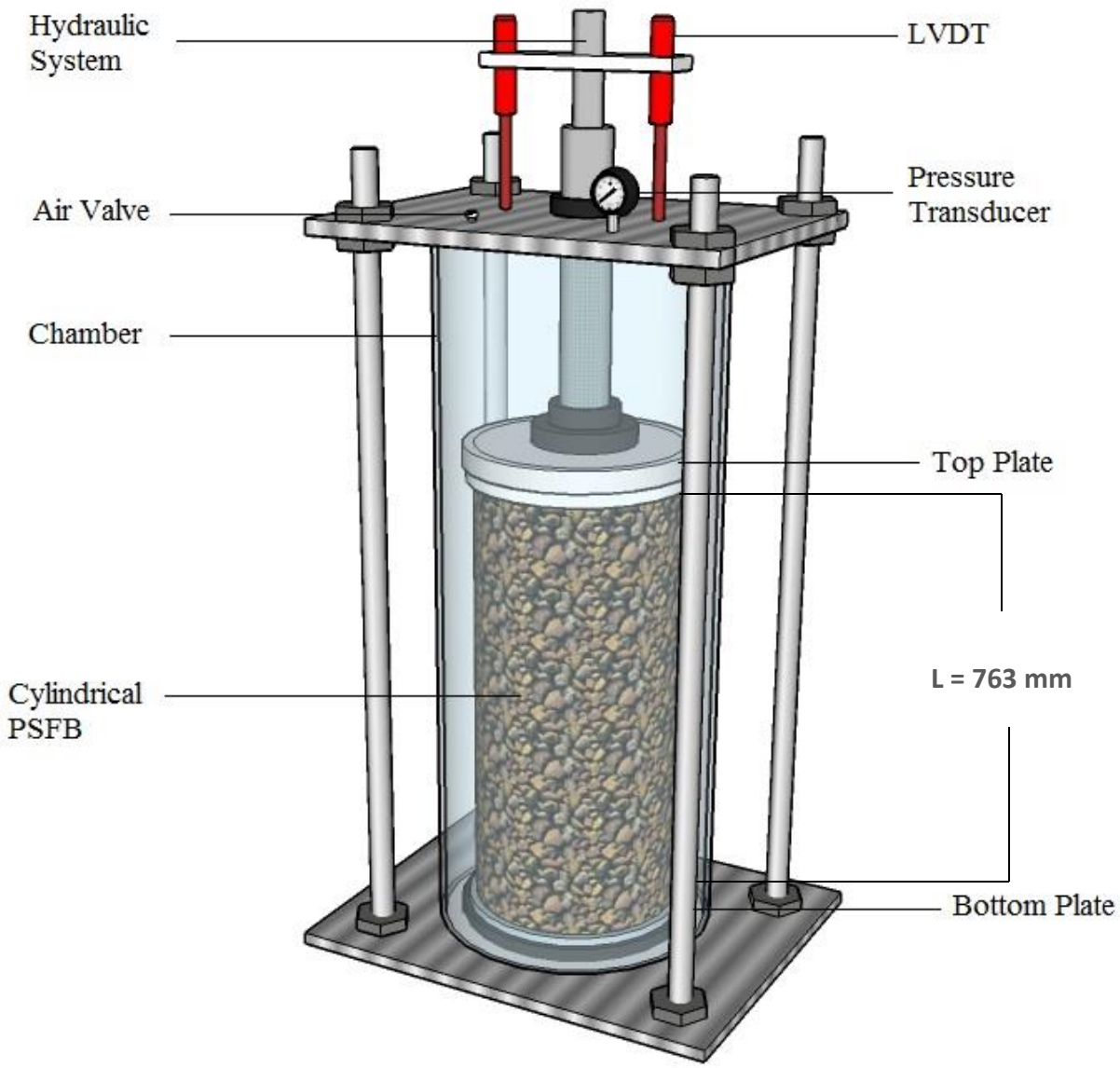

Figure 4.3 Cyclic - Triaxial Compression Chamber

4.3.2 Analysis of Cyclic Triaxial Compression Tests

The cyclic triaxial compression test consists of applying a constant confining pressure (σ_3) to a specimen that is contained within a membrane and sealed in a triaxial chamber. A plunger or piston that extends through a seal in the top plate of the triaxial cell applies the cyclic load. The methodology described by Ebrahimi et al., (2011) was followed. The cyclic load is applied as a 5-Hz haversine, bell-shaped loading pulse with peak and rest loads as used in the large-scale cyclic triaxial tests using a deviator stress, σ_d of 350 kPa, and a confining pressure, σ_3 of 100 kPa with 200,000 loading cycles for each specimen as recommended by Ebrahimi et al. (2011). Lichtberger (2005) reported that the pressure at the top of the ballast layer was as high as 370 kPa, Aursudkij et al. (2009) conducted tests on clean ballast up to a cyclic deviator stress of 360 kPa to determine deformational response; however, in their study, they determined that stresses up to 260 kPa were typical from rail loading. Table 4.1 shows that stress distribution on railway under different car loading (Talbot 1980; Ebrahimi et al. 2011). Considering these studies, 350 kPa was considered which is the middle range from typical rail loading.

Table 4.1 Stress Distribution on Railway System (Talbot 1980; Ebrahimi et al. 2011)

Rail Car Gross Weight (kg)	Deviator Stress, σd (kPa)	Confining Pressure, σ3 (kPa)
88.100	250	90
101.151	300	90
114.305	350	90
127.006	400	90
140.160	450	90

$$\sigma_p = \frac{F_P}{A_P} \qquad \text{Eq. (4.4)}$$

where the load from the piston (F_p) is applied through the area of the plate on top of the specimen (A_p). After each loading cycle, a non-recoverable deformation (plastic deformation, δ_p) is measured and plastic strain ε_p calculated from

$$\varepsilon_p = \frac{\delta_P}{L} \qquad \text{Eq. (4.5)}$$

where L is the original length of the specimen. Throughout the cyclic triaxial test, plastic strain accumulates, which provides the deformational behavior of a material over the life cycle of loading cycles.

4.4 Elastic Wave (Non-Destructive Seismic) Test

4.4.1 **Methodology**

Elastic wave (seismic) tests were conducted on PSFB cylindrical samples to compare to results obtained from cyclic-triaxial compression testing on PSFB cylindrical samples in order to verify the deformation in PSFB cylindrical samples. Elastic wave testing methods are commonly used for field and laboratory investigations as non-destructive determination of the stiffness of materials. Testing was conducted (ASTM C 215 and ASTM C 1198) using a PCB-086C01 impact-hammer used for wave excitation and the signal was measured using a PCB-353B16 ICP Accelerometer. Signal acquisition was done through a Tektronix 2041 oscilloscope and data recorded using Tektronix OpenChoice Desktop software.

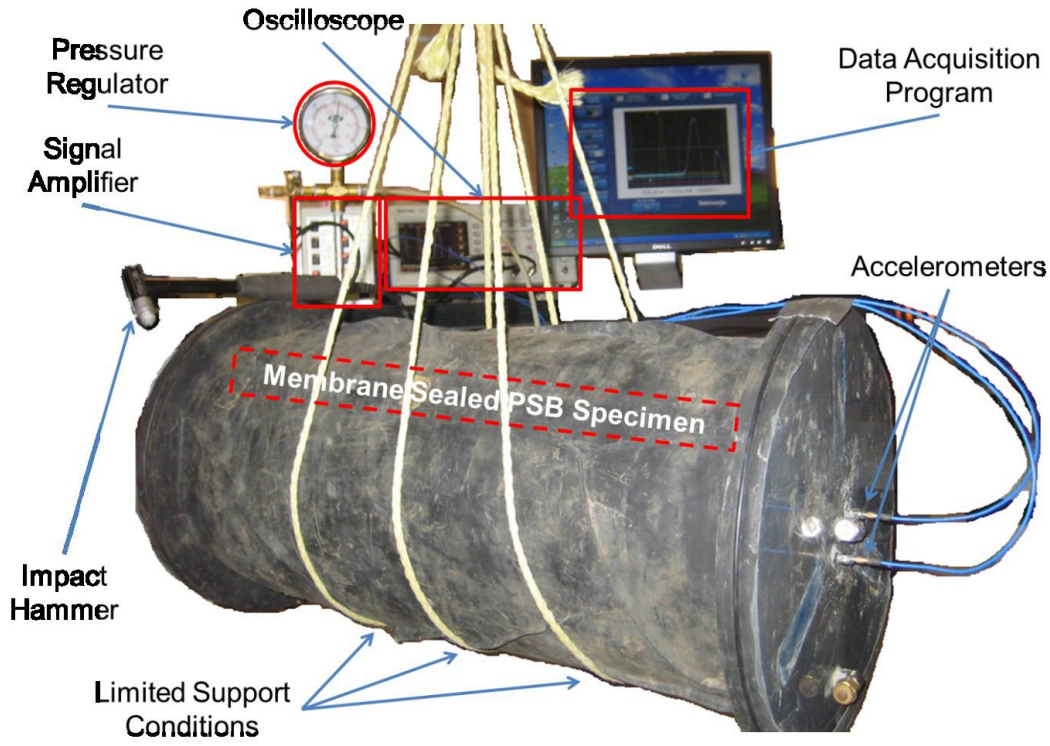

Figure 4.4 Picture of Membrane-Sealed PSB Specimen Subjected to Small-Stain Elastic-Wave Based Testing after Keene et al. (2012).

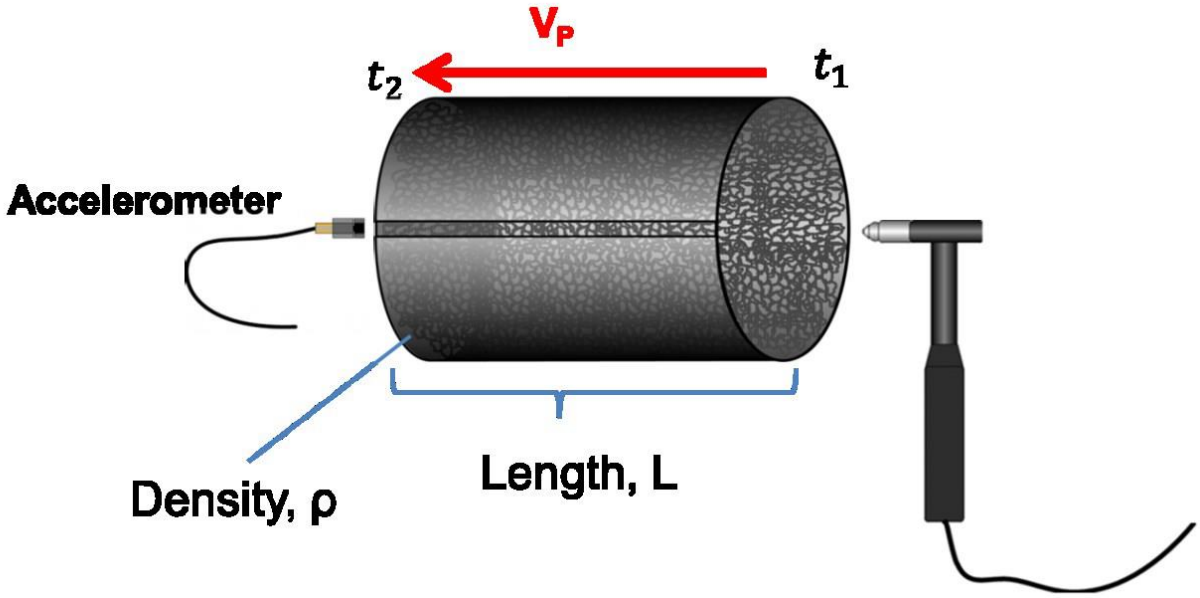

Figure 4.5 Small-Strain Elastic Wave Testing Approach after Keene et al. (2012)

4.4.2 Analysis of Elastic Wave test

Knowing the travel time of the signal through the material and bulk density, a seismic modulus can be calculated. From a measurement of the p-wave travel time, the p-wave velocity (VP) is calculated by

$$Vp = \frac{t2-t1}{L} \qquad \text{Eq. (4.6)}$$

where t1 is the time of p-wave excitation, t2 is the p-wave arrival time, and L is the length of the specimen. With VP and specimen bulk density (ρB) known, the constrained modulus (M) is calculated by

$$M = V_p^2 \rho_B \qquad \text{Eq. (4.7)}$$

Where Vp is p-wave velocity (m/s), ρB is the bulk density of PSB (kg/m3).

5. RESULTS AND DISCUSSIONS

5.1 Mechanical Behavior of PSFB and PSB beams under Monotonic Flexural Loading

Monotonic-flexural loading test is used for determining flexural strength of bound materials that undergo repetitive bending in transportation infrastructure, such as concrete, asphalt, and cement-stabilized soils. In this research, flexural loading testing method was used to obtain mechanical properties of PSFB and PSB beam specimens. Four PSFB and one PSB beams were prepared and tested in the third-point configuration. They were loaded through a servo-hydraulic system (MTS®, loading capacity of ~22 kN). Similar behavior was observed in the five beams, where deflection increased linearly and there was little warning before failure (i.e., brittle failure in monotonic flexural loading), as evidenced in Figure 5.1. The results of the five beams are summarized in Table 5.1. The PSB beam specimen (FI = 0% WC = 0%) has the highest flexural strength (rupture modulus) of 1582 kPa while the PSFB specimen with the highest fouling (FI = 15%) and water content (WC = 13%) has the lowest flexural strength of 311 kPa.

When the WC and FI increase, the strength of PSFB decreases significantly. Increasing (FI) decreases the strength of PSFB by affecting the condition of the ballast particle contact points by the fouling material.. Fouling materials at the contact points of ballast particles cause weakness in the ballast skeleton and accelerates the accumulation of plastic strains (Selig and Water 1994). Mineral fouling derives from ballast particles breaking down under cyclic loading and it is present at the ballast particle contacts and fills out the ballast voids. The fouling material in ballast voids increase the shear strength and stiffness of the ballast (Selig and Water 1994). Because the fouling material affects the ballast skeleton if the fouling material coats the ballast particle surface based on (Selig and Water 1994). However, fouling materials move with water

between the ballast particles and coat the surface of ballast. When the ballast surface coated with fouling material, the polyurethane does not bond well during the RPF reaction. This is shows how water content (WC) has very important role in fouled ballast.

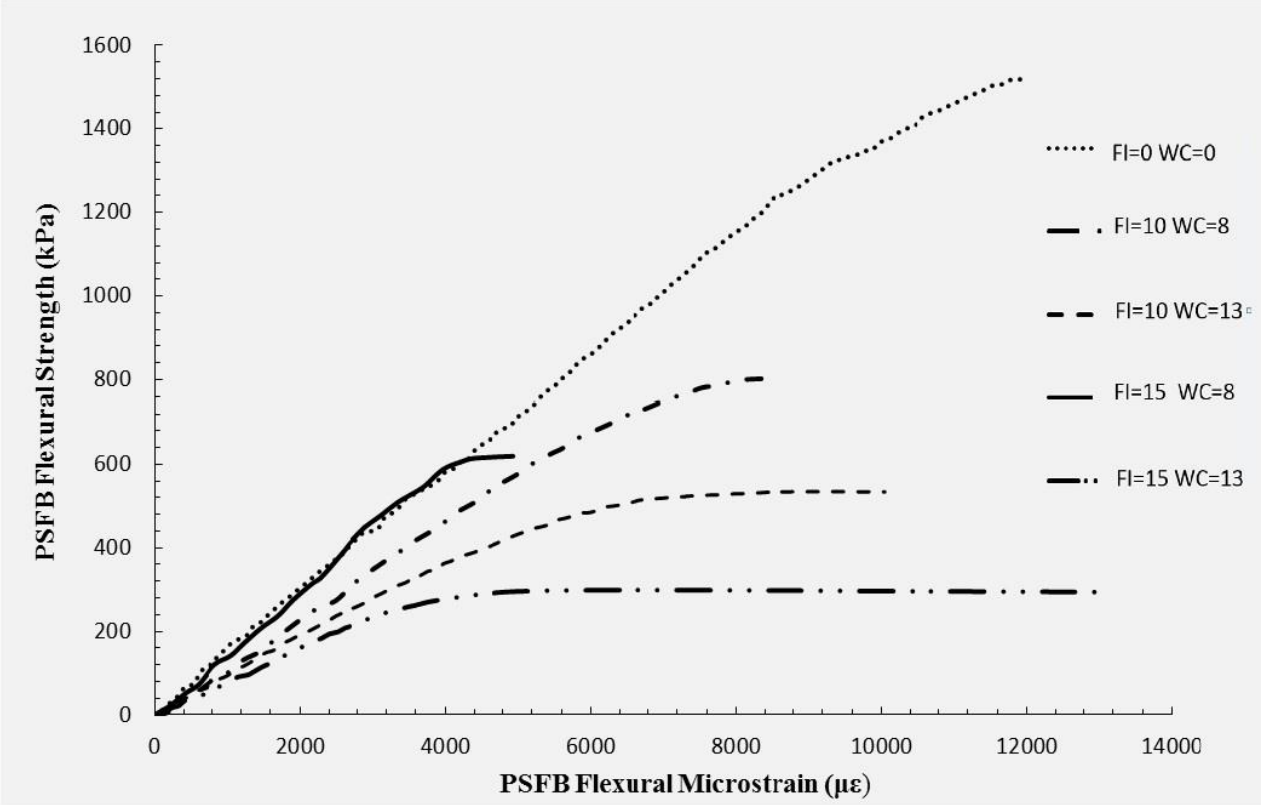

Figure 5.1 Flexural Strength Tests Conducted on four PSFB and one PSB Beams with Different FI (%) and WC (%)

Table 5.1 Rupture Modulus for PSFB and PSB Beams Samples

Beams FI and WC	**Rupture Modulus (kPa)**
FI = 0% - WC = 0%	1582 kPa
FI = 10% - WC = 8%	843 kPa
FI = 10% - WC = 13%	562 kPa
FI = 15% - WC = 8%	731 kPa
FI = 15% - WC = 13%	311 kPa

5.2 Mechanical Behavior of PSFB and PSB Prismatic Specimens under Unconfined Compression Strength (UCS) Test

After the monotonic flexural test, the four PSFB and one PSB beams were ruptured near the mid-length. These PSFB and PSB beam specimens were cut with a concrete masonry saw to the height to width ratio of 2:1 which are called "prisms" in this study. This dimension was established in Keene et al. (2012) to reduce the effect of friction on the specimen. As shown in Fig. 5.2, highest unconfined compressive strength (q_u) of 2850 kPa is reached by the PSB (FI = 0% WC = 0%). The highest fouling (FI = 15%) and water content (WC = 13%) in the PSFB yielded a (q_u) o□ around 1763 kPa. The failure mode observed during testing was a delamination with the RPF foam stripping away from the rocks and a ductile failure.

Elastic modulus depends on PSFB prism density, as shown in Fig. 5.3. PSFB which has a highest density (1875 kg/m^3) has the lowest elastic modulus (65 MPa). As the overall (bulk) density of PSFB increases, there was a linear decrease in elastic modulus. The more fouling material introduced into the ballast matrix, a less rigid material resulted. With increased fouling, decreased PU-ballast bonds result, and the less stiff fouling material transmits increased load.

However PSB samples which were tested in UCS in previous research determined when the PSB density increased the elastic modulus increased as well (Keene et al. 2012). Because PSB includes only ballast and PU, a more rigid material can be expected with additional ballast and added aggregate interlock. Concrete exhibits the same behavior in UCS as PSB, as the design strength and concrete density increases; the elastic modulus increases (Grider et al. 1999).

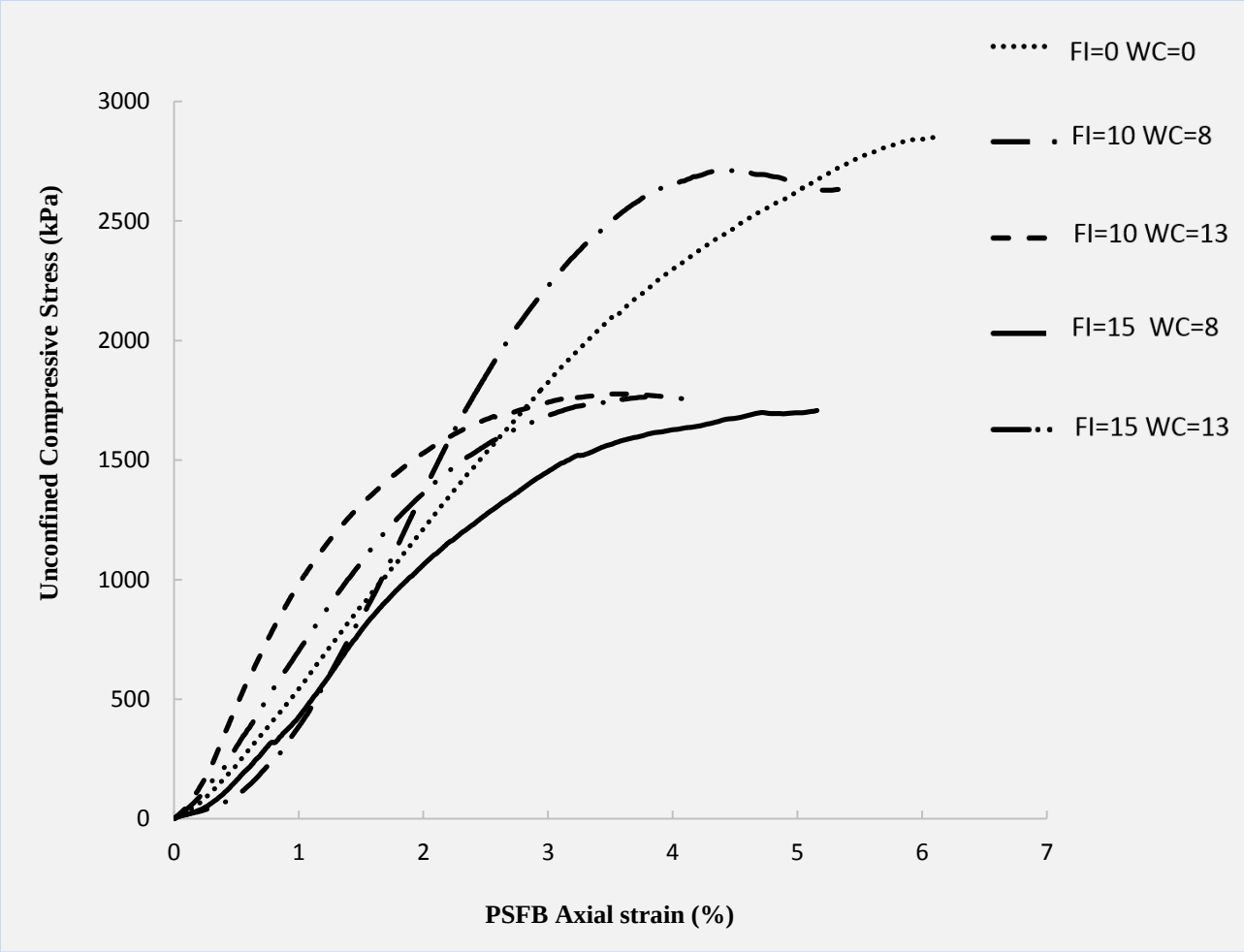

Figure 5.2 Unconfined Compression Strength Tests Conducted on Five PSB Prisms with Different FI (%) and WC (%)

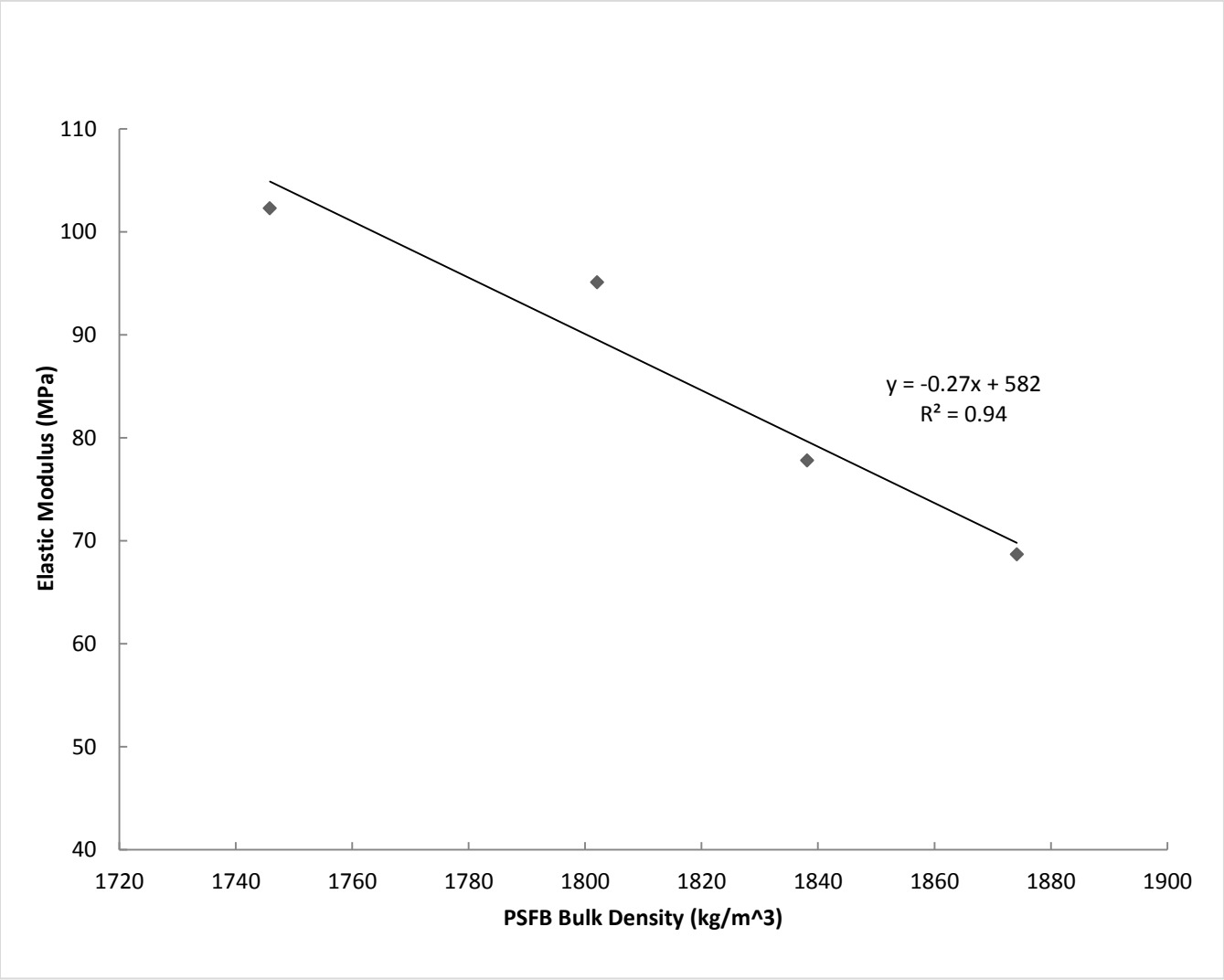

Figure 5.3 Elastic Modulus Obtained from PSFB Prism UCS Tests Compared with PSFB Prism Density.

Fig 5.4 compares the average PSFB flexural and compressive strengths of all specimens with those of PSB and clean ballast from other studies by Keene et al. (2012)) and Ebrahimi et al. (2011). Unstabilized clean ballast strength result was taken from cyclic triaxial tests conducted by Ebrahimi et al., (2011), where the confining pressure, σ_3 was 100 kPa. . Average monotonic flexural strength of PSB (938 kPa) is about 35% greater than the average monotonic flexural strength of PSFB (611 kPa). The average UCS strength of the PSB specimens (3200 kPa) is greater than that of the PSFB specimens (2713 kPa). However, PSFB has a greater strength (about 74%) than unstabilized clean ballast. Fig. 5.5 shows that elastic modulus of PSFB, PSB, and clean ballast. Clean ballast has higher elastic modulus than PSFB and PSB, although it is unstabilized, because it is an angular granular material with mineral particle contacts. After the RPF injection procedure, the clean ballast elastic modulus decreases from 275 MPa to 98 MPa as polyurethane enters the ballast particle contacts. PSFB has higher elastic modulus than PSB because of high percentage of polyurethane weight in PSB.

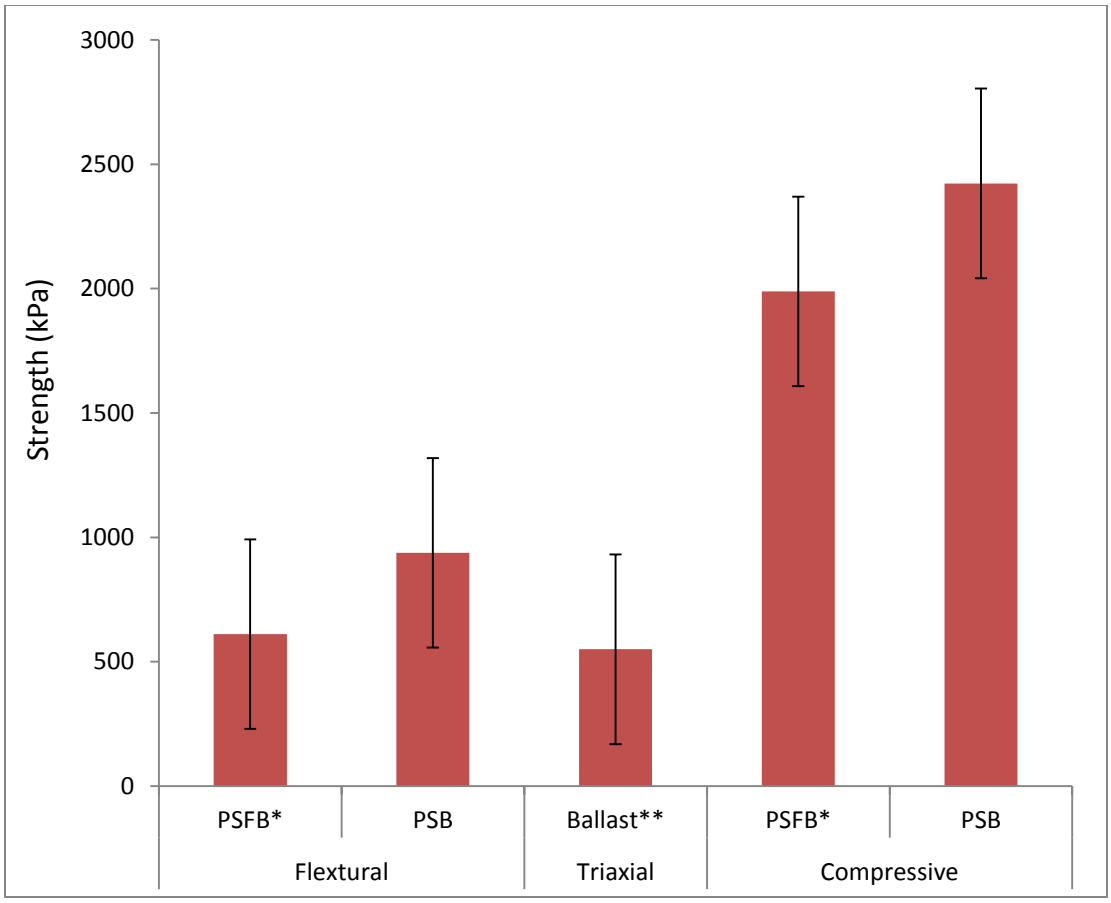

Figure 5.4 Flexural and UCS Tests Comparison of Results for PSFB* and PSB

*** PSFB presents a different FI% and WC% samples**

**** Representative ballast compressive strength was taken where confining pressure, σ3 was 100 kPa.**

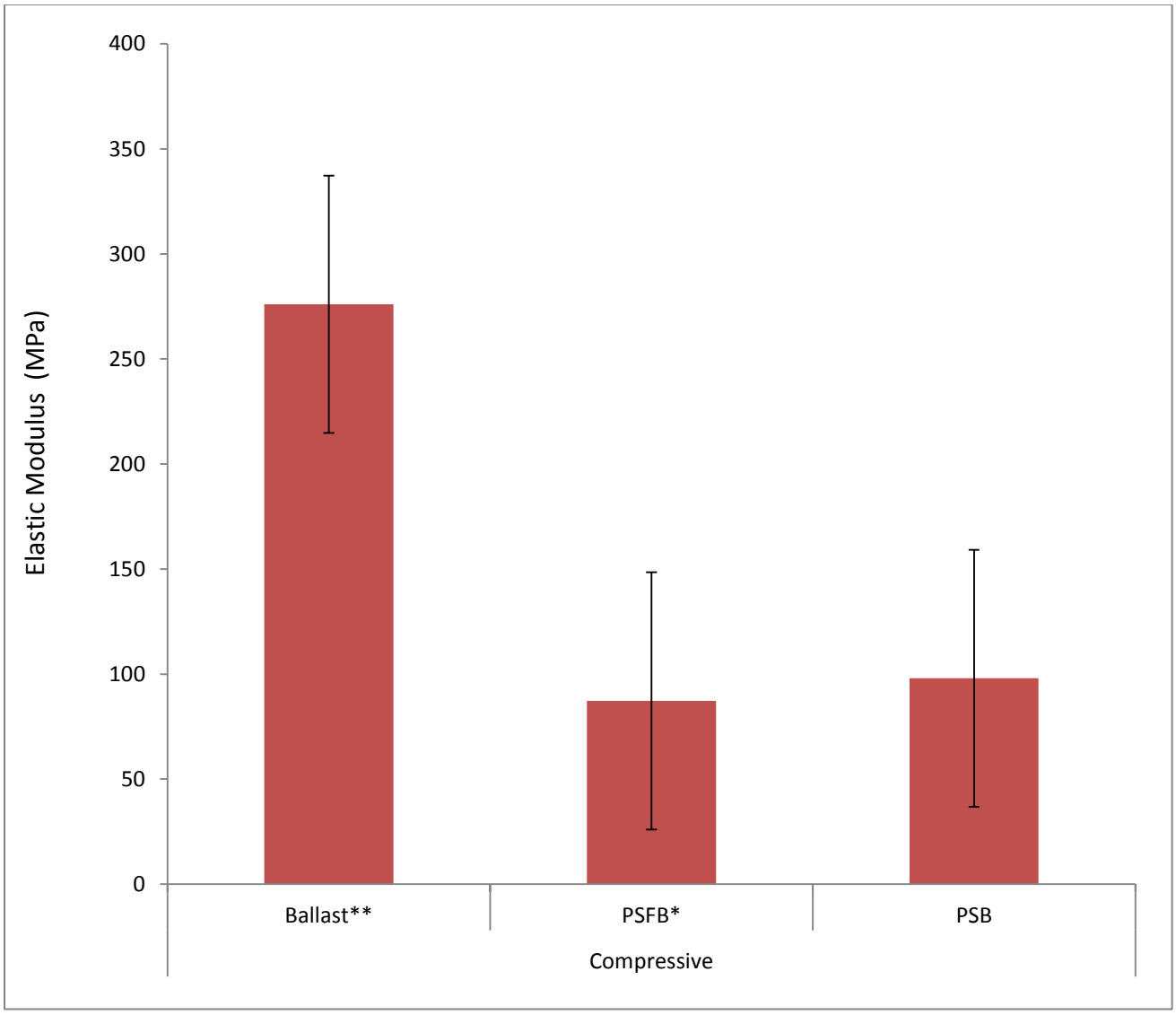

Figure 5.5 UCS Test Elastic Modulus Comparison of PSFB*, PSB and Clean Ballast

*** PSFB presents a different FI% and WC% samples**

**** Representative ballast Elastic Modulus was taken where confining pressure, σ3 was 100 kPa.**

5.3 Behavior of PSFB and PSB in Cyclic-Triaxial Compression Tests

Cyclic triaxial compression tests were conducted for determining the plastic deformational behavior of cylindrical PSFB and PSB specimens. Plastic strain of PSFB was measured as a function of cycles for a different range of fouling indices (FI) and water contents (WC). Cyclic-triaxial testing of ballast and railway materials has been reported in previous studies Ebrahimi et al. (2011) and Keene et al. (2012). After 200,000 load cycles, the data was analyzed for plastic strain.

For all of the specimens, the plastic strain at the end of the test was under the Federal Rail Administration (FRA) limit for maintenance (2.5-3%) Hesse (2013) and Keene et al. (2012). There is significant improvement in resiliency of the polyurethane stabilized ballast compared to non-stabilized fouled ballast. As shown in the Fig. 5.6 below, specimens of similar fouling type and water contents show drastic improvement in developed plastic strain. During RPF reactions, polyurethane fills the fouled ballast voids and makes the fouled ballast specimen stronger, which reduces the plastic strain and strength under cyclic loading. Accumulation of plastic strain in PSFB and PSB can be attributed to two possibilities: (1) ballast particle breakage and localized rearrangement of fractured ballast particles (i.e., movement of fractured particles within the RPF encasement) or (2) frictional wear and foam degradation due to the interaction of fragmented ballast and RPF (Keene et al 2012). However, after the injection, the polyurethane fills ballast voids and prevents: (1) ballast particle breakage, (2) relocation of ballast particles, (3) friction wear of particles.

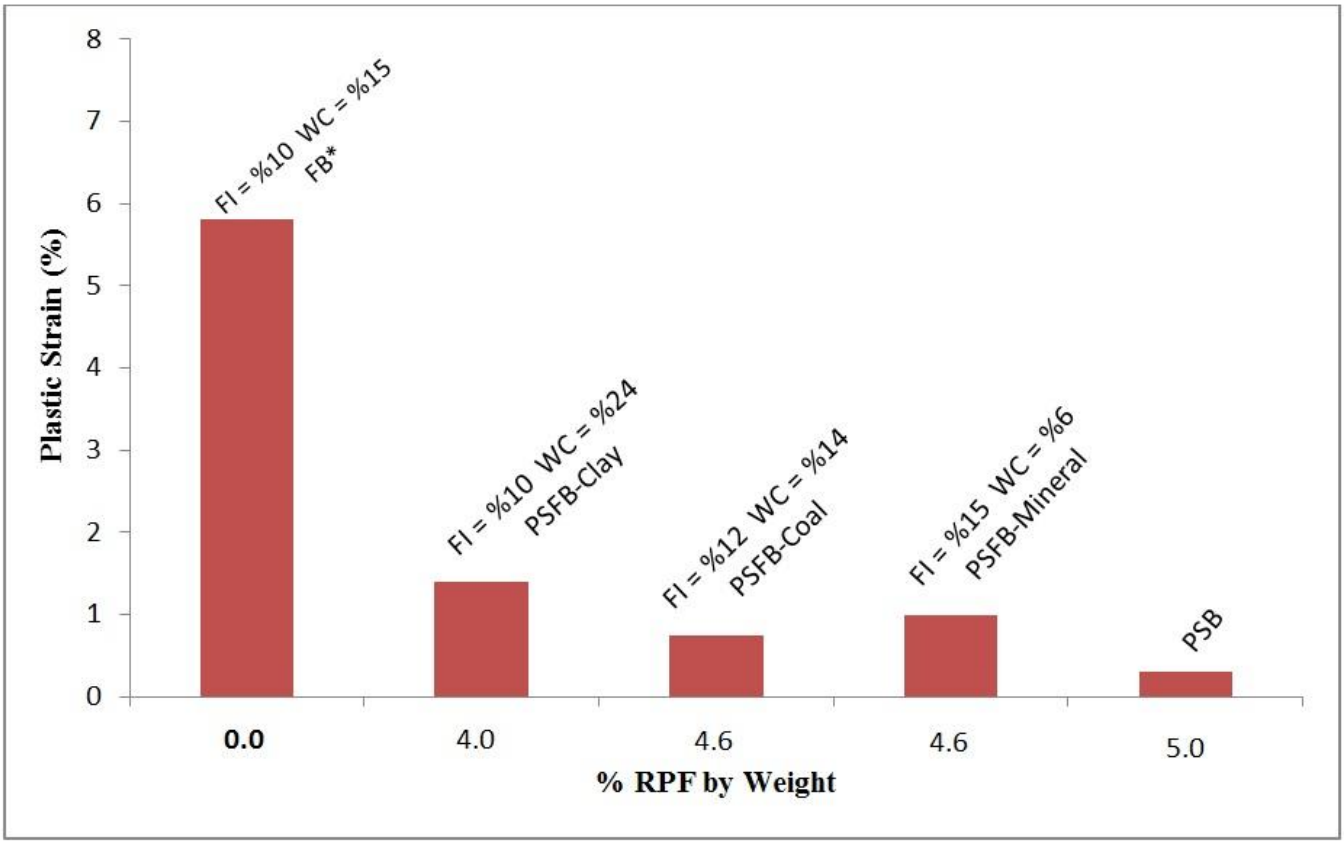

Figure 5.6 Plastic Strain Over 200,000 Cycles

*Fouled Ballast

5.3.1 Polyurethane Stabilized Coal Fouled Ballast (PSFB-CO)

Injection of polyurethane into a coal fouled ballast matrix reduces plastic strain (50% - 81%) over 200,000 loading cycles. The rate of plastic deformation of PSFB increases continually with increasing cycles of loading in semi-log scale (see Fig. 5.8). The PSFB-CO cylindrical specimen with the highest FI (24%) and WC (14%) has the highest plastic strain of 1.02%. By increasing WC and FI, the plastic strain $\varepsilon_{\square}$ increases significantly (50%). Increasing FI increases the plastic strain of PSFB by affecting the condition of the contact points of large ballast particles. Fouling interacting with the contact points of ballast particles reduces the shear resistance properties of the ballast skeleton and accelerates the accumulation of plastic strain. According to Polito and Martin (2001) when the voids created by large particles are filled by fines but the contact points of particles are intact, the strength and deformational properties of the mixture is not influenced by the presence of fines. If fines coat the contact points of large particles, an unstable structure may develop that may decrease the strength of the original particle network. Another effect of fouling is that when fouling material coates the surface of ballast, the polyurethane does not bond well with ballast particles during the RPF reaction. Water content (WC) has a very important role in fouled ballast. Ebrahimi et al. (2011) stated that non-cohesive fouling materials (coal and mineral fouling) by itself does not affect the ε_p of ballast when fouling is nearly dry ($w < 3\%$). This behavior might be due to (1) retention of relatively clean contact points of ballast at low water condition and (2) higher strength properties of dry non-cohesive fouling in contact points of ballast; i.e., binding ballast particles. When water content (WC) increase in fouled ballast, fouling materials move and the ballast particles are coated with fouling material, lubricating the ballast particles resulting in a weakened structure. Furthermore, when the fouling material becomes wet, excess pore water pressure develops

between fine particles during cyclic loading, resulting in a weaker ballast structure (Selig and Waters 1994). Excess pore pressure refers to a sudden increase in pore pressure within a soil due to rapidly applied loading conditions. Materials with low permeability such as clays, may exhibit this behavior (Skempton, 1954). Effective stress depends on applied stress and pore water pressure. When the fouling material becomes wet, pore pressure increases and the effective stress decreases which may cause the ballast skeleton weakness. Figure 5.7 shows excess pore pressure under cyclic loading.

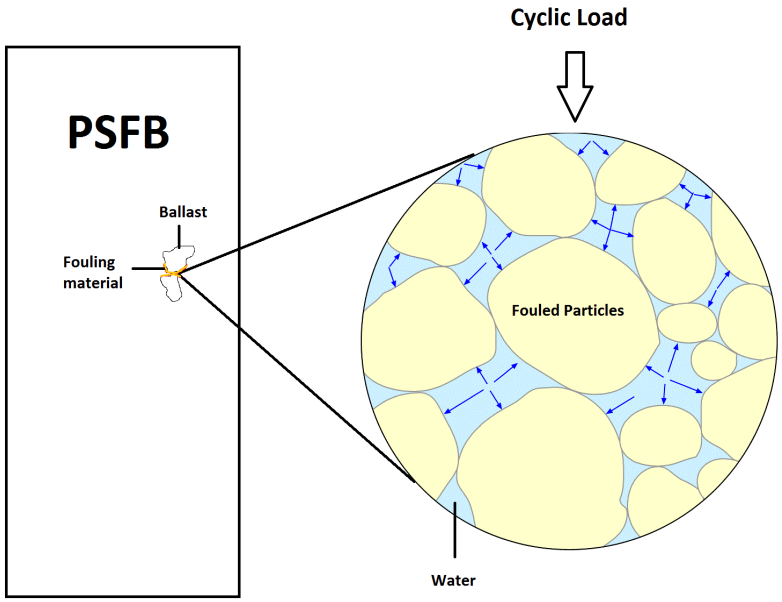

Figure 5.7 Excess pore pressure in PSFB specimen

The water between fouled particles RPF injection with varying fouling indices (FI) and water contents (WC) impact strength and plastic strain in coal fouled ballast in different ways depending of the polyurethane weight. The figure 5.9 shows percentage of polyurethane weight in PSFB-CO with different FI and WC. Highest FI in PSFB-CO has the lowest percentage of

polyurethane weight because fouling materials fill out the ballast voids and leaving smaller voids filled with the RPF.

There was a significant reduction in final plastic strain of PSFB-CO relative to the findings of Ebrahimi et al. (2011) with similar but unstabilized FB-CO (Coal Fouled Ballast) specimens as presented in Fig. 5.10. The unstabilized fouled specimens that were used in the comparison were tested at a deviator stress of 300 kPa whereas the PSFB-CO was tested at 350 kPa. One can expect that if tested at higher stresses more deformation would occur. The results show that polyurethane injection method improves the ballast structure and reduce the plastic strain. After RPF injection procedure, coal fouled ballast (FI = 24% WC = 8%) plastic strain decreased 1.35% to 0.59%, which is 75% reduction. Since polyurethane fills the ballast voids and reduce the plastic strain of ballast. Table 5.2 shows coal fouled ballast reductions after RPF injection method.

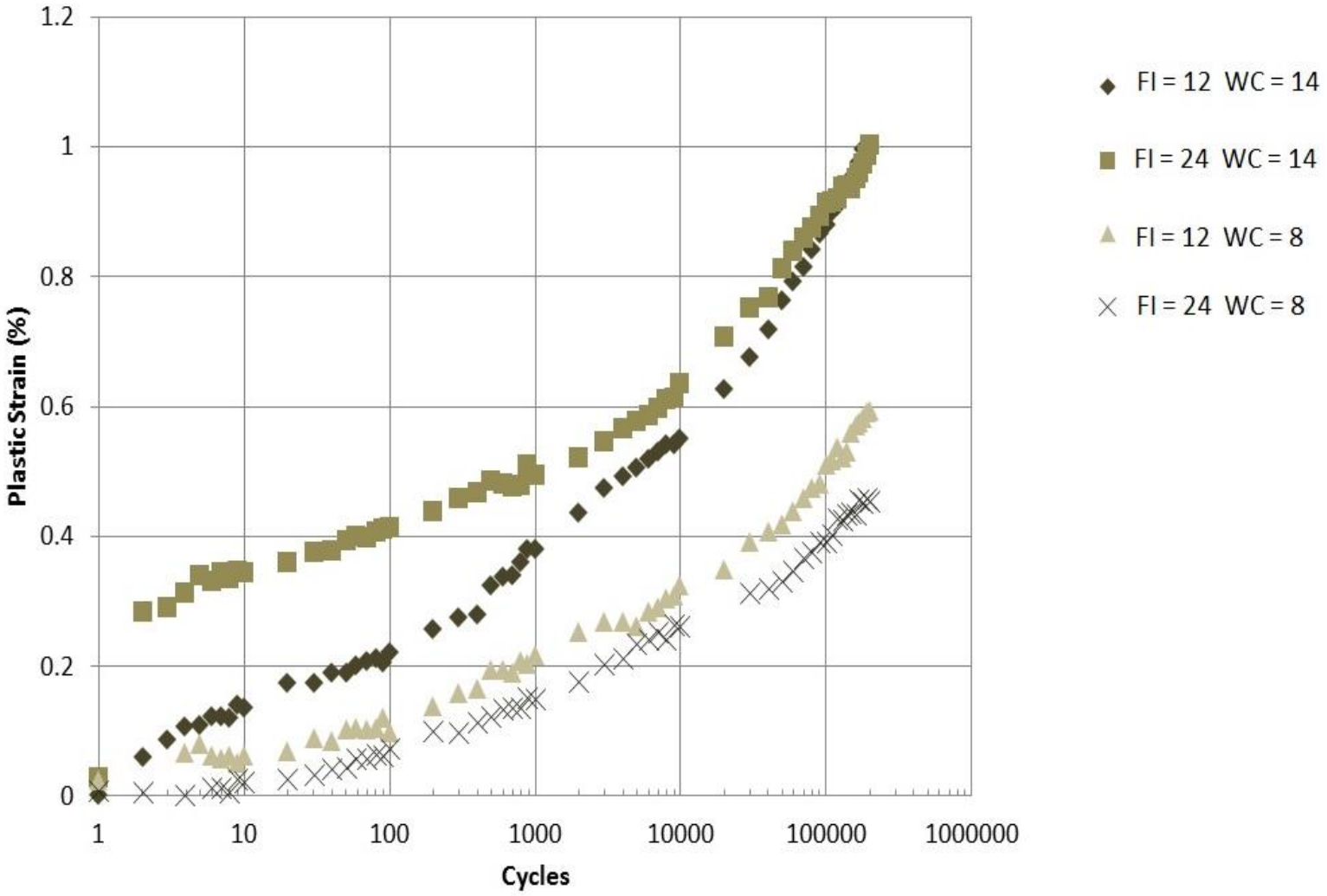

Figure 5.8 The Results of Large-Scale Cyclic- Triaxial Compression Tests On PSFB-CO Specimens

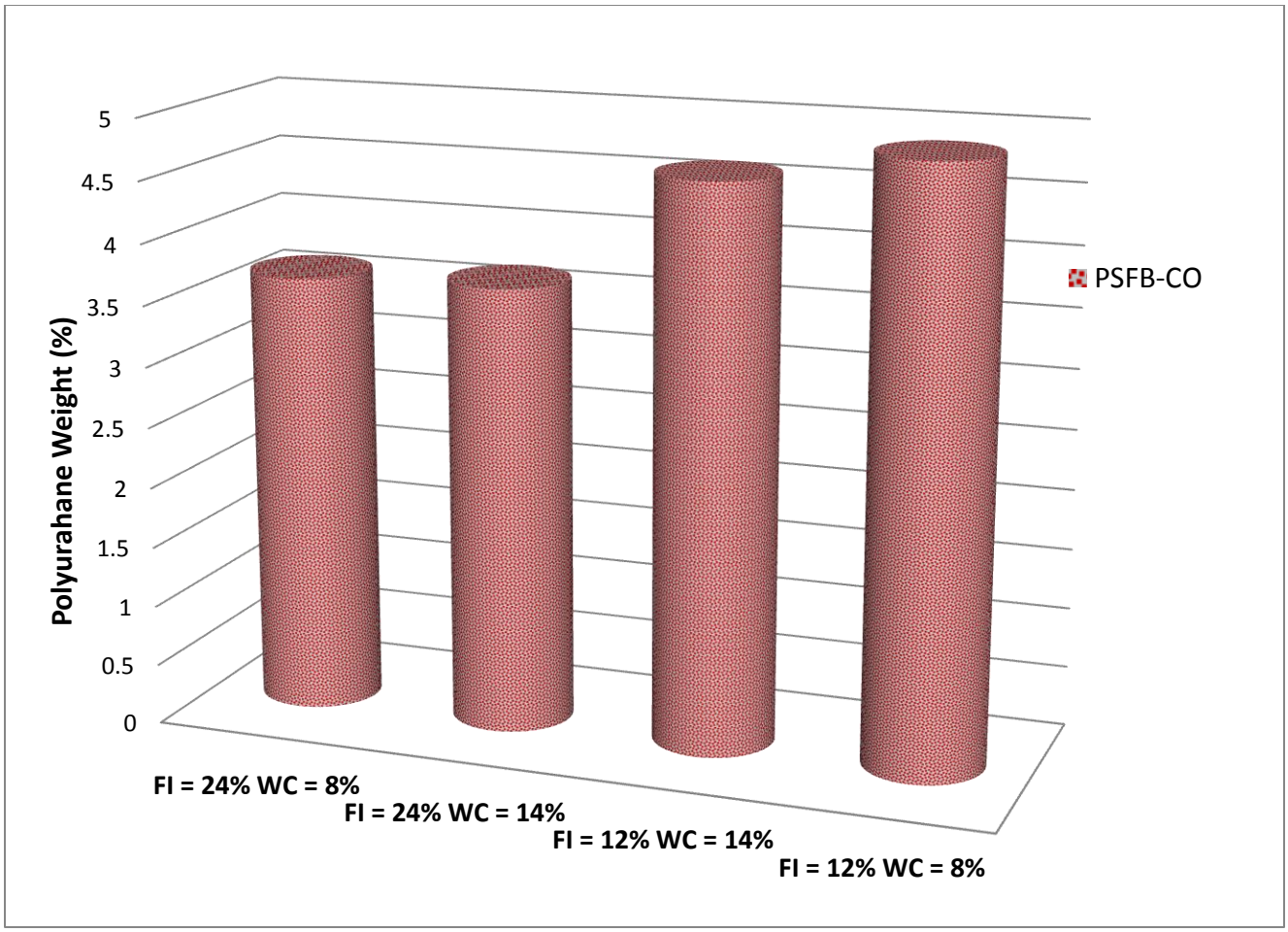

Figure 5.9 Percentage of Polyurethane Weight in PSFB-CO with Different FI and WC

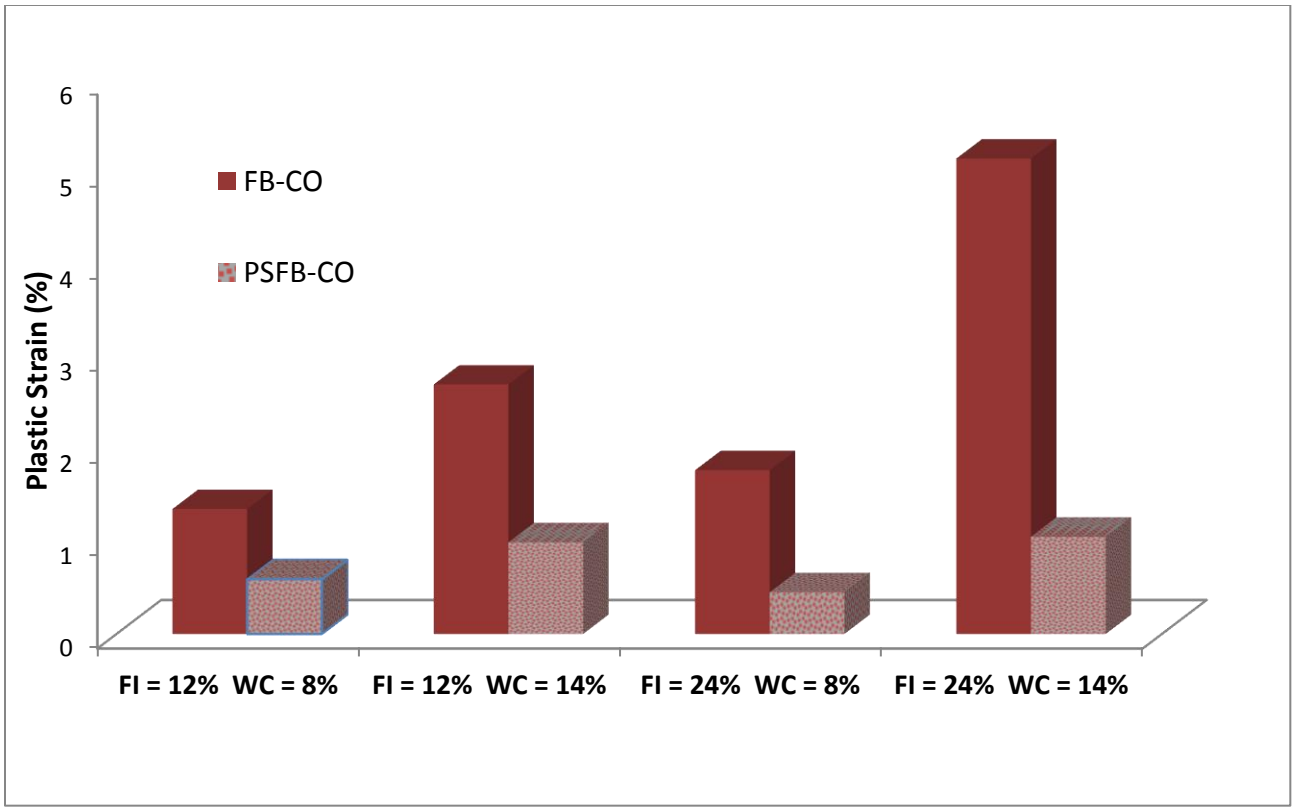

Figure 5.10 Plastic Strain Distribution Between PSFB-CO and FB-CO (Coal Fouled Ballast) Over 200,000 Cycles

Table 5.2 Comparison of Plastic Strain Between PSFB-CO and FB-CO (Coal Fouled Ballast)

Sample Description	**PSFB-CO Plastic Strain**	**FB Plastic Strain** Ebrahimi et al. (2011)	**Reduction**
FI = 12% WC = 8%	0.59%	1.35%	56%
FI = 12% WC = 14%	0.99%	2.70%	63%
FI = 24% WC = 8%	0.45%	1.77%	75%
FI = 24% WC = 14%	1.02%	54.15%	75%

5.3.2 Polyurethane Stabilized Clay Fouled Ballast (PSFB-C)

Injection of polyurethane into a clay-fouled ballast matrix reduced the plastic strain by a considerable amount over 200,000 loading cycles (see Fig. 5.11). The PSFB-C beam specimen (FI = 20% WC = 14%) has the highest plastic strain of 1.46% while the PSFB-C specimen with the lowest fouling (FI = %10) and water content (WC = 24%) has the lowest plastic strain of 1.33%. When the FI and WC increase in PSFB, plastic strain of PSFB decreases. Plastic strain of PSFB-C mainly depended on FI and WC as well as non-cohesive fouling materials such as coal, mineral fouling and frac sand. However, PSFB-C specimens response did not depend on just FI and WC. Clay mineralogy played significant role in the PSFB-C specimens. Clay is cohesive fouling material and Fig. 5.12 shows that a PSFB-C specimen has higher average plastic strain than non-cohesive PSFB because of high plasticity of clay (kaolinite). Vanapalli et al. (1996) described that an increase in WC of clay decreases the shear strength.

The clay used to prepare these samples has a liquid limit and plasticity index comparable to the one used by Ebrahimi et al. (2011) in testing unstabilized clay-fouled specimens. Tests on PSFB-C were conducted in a manner similar to the tests by Ebrahimi et al. (2011) and a low deviator stress (300 kPa) was used (Fig. 5.13). After RPF injection procedure, plastic strain decreased 5.45% to 1.46% in clay fouled ballast (FI = 20% WC = 14%), which is 73% reduction (see Table 5.3).

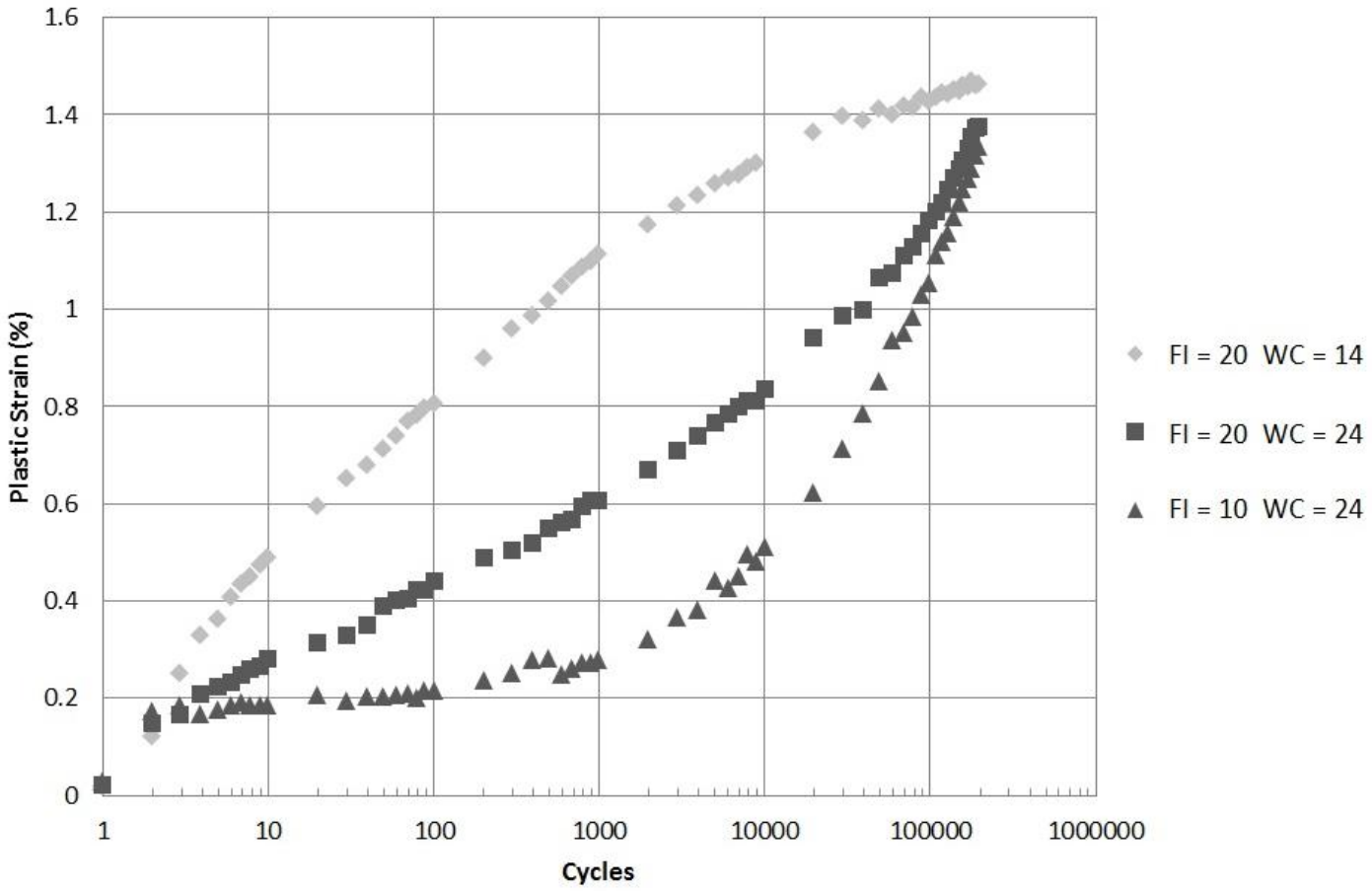

Figure 5.11 The Results of Large-Scale Cyclic - Triaxial Compression Tests on PSFB-C Specimens

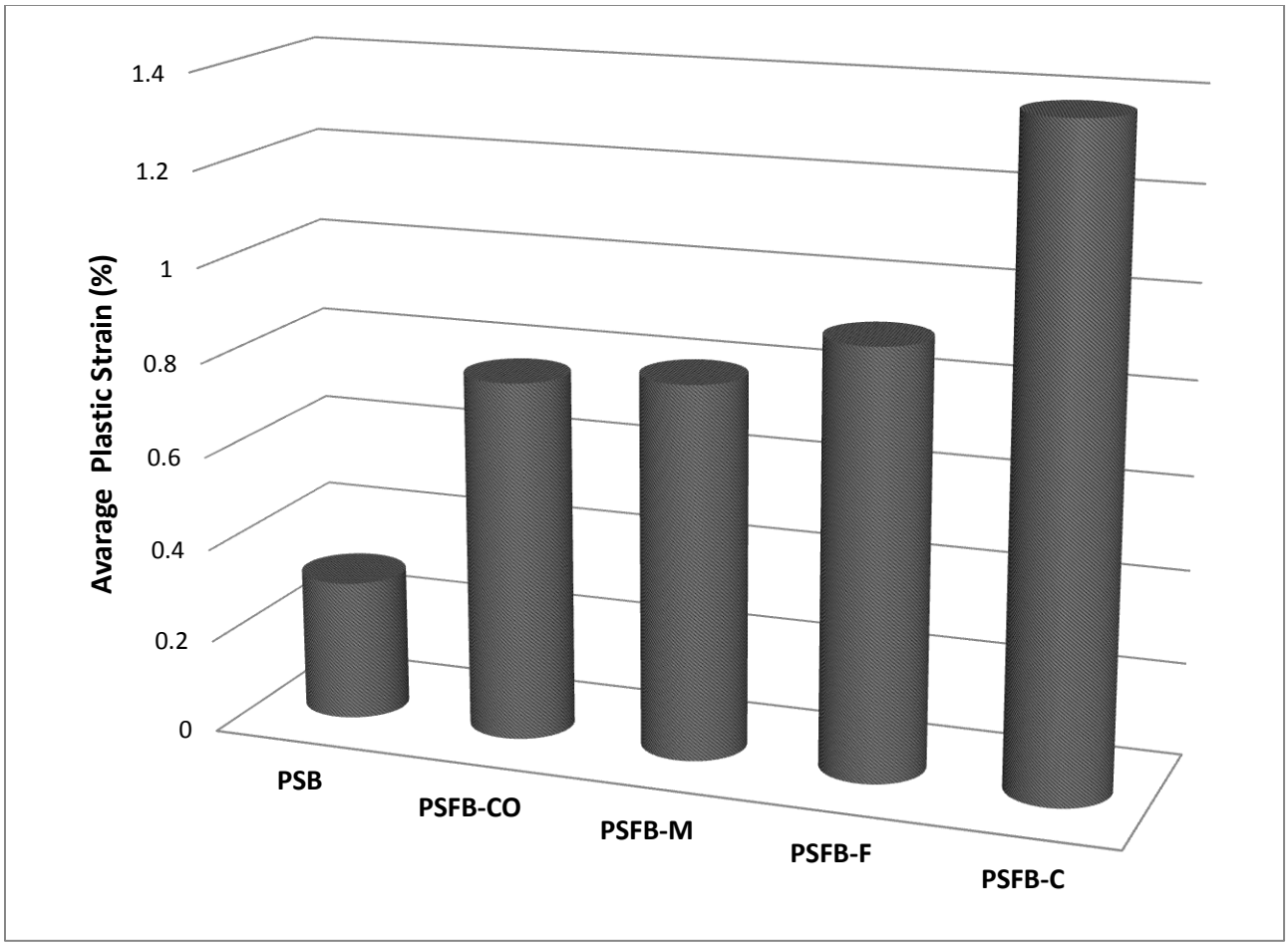

Figure 5.12 Average Plastic Strain Distribution Between PSB, PSFB-CO, PSFB-M, PSFB-F and PSFB-C Over 200,000 Cycles

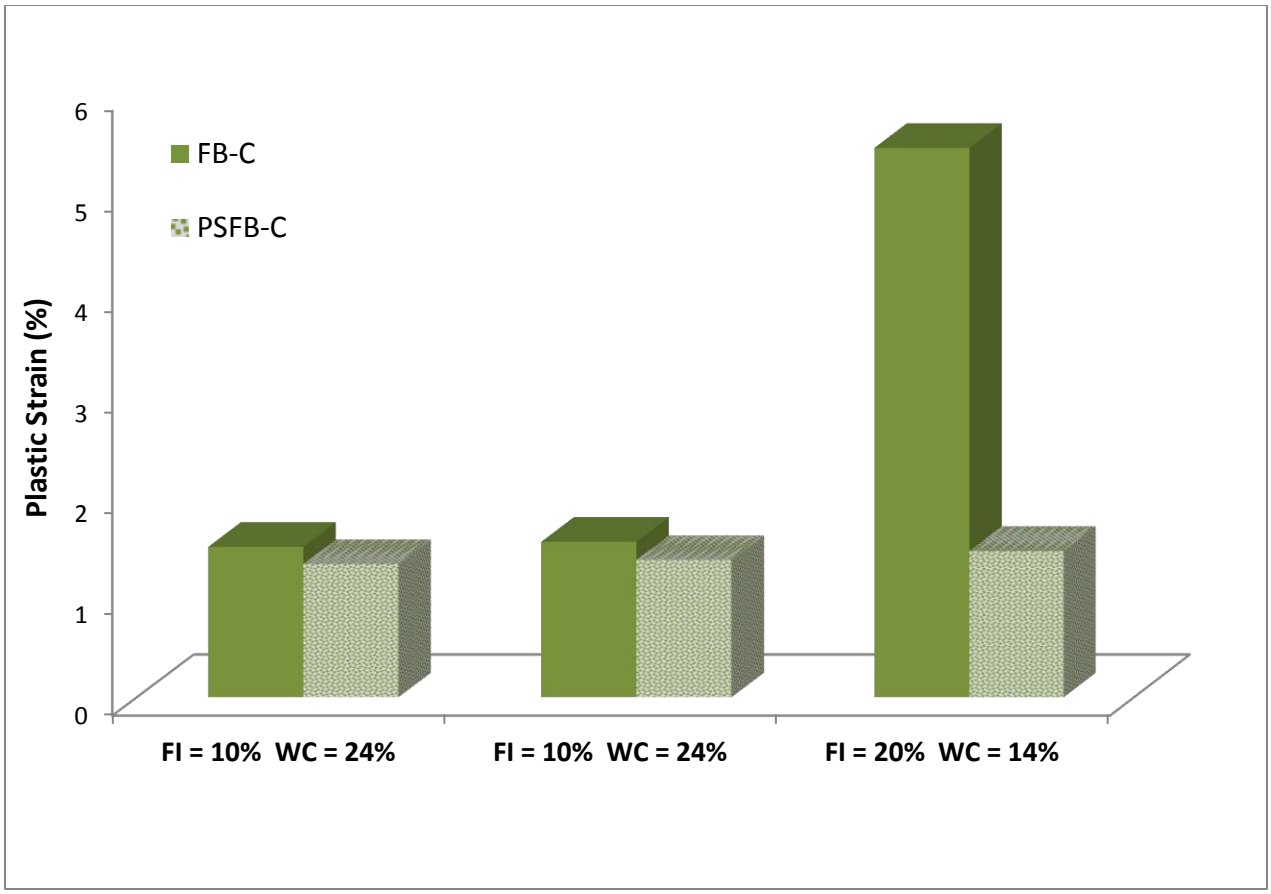

Figure 5.13 Plastic Strain Distribution Between PSFB-C and FB-C (Clay Fouled Ballast) Over 200,000 Cycles

Table 5.3 Comparison of Plastic Strain Between PSFB-C and FB-C

Sample Description	PSFB-C Plastic Strain	FB-C Plastic Strain Ebrahimi et al., 2011	Reduction
FI = 10% WC = 24%	1.33%	1.50-1.60%	11-17%
FI = 10% WC = 24%	1.37%	1.50-1.60%	9-15%
FI = 20% WC = 14%	1.46%	5.45%	73%

Figure 5.14 shows percentage of polyurethane weight in PSFB-C with different FI and WC. Two PSFB-C specimens were prepared with the same FI and WC to determine the variation induced induced by sample preparation. There is just 1.2% of RPF weight difference which can be ignored.. When the fouling material increases in the PSFB-C, percentage of polyurethane weight decreases because increasing fouling material fills the voids and leaving smaller space for the polyurethane.

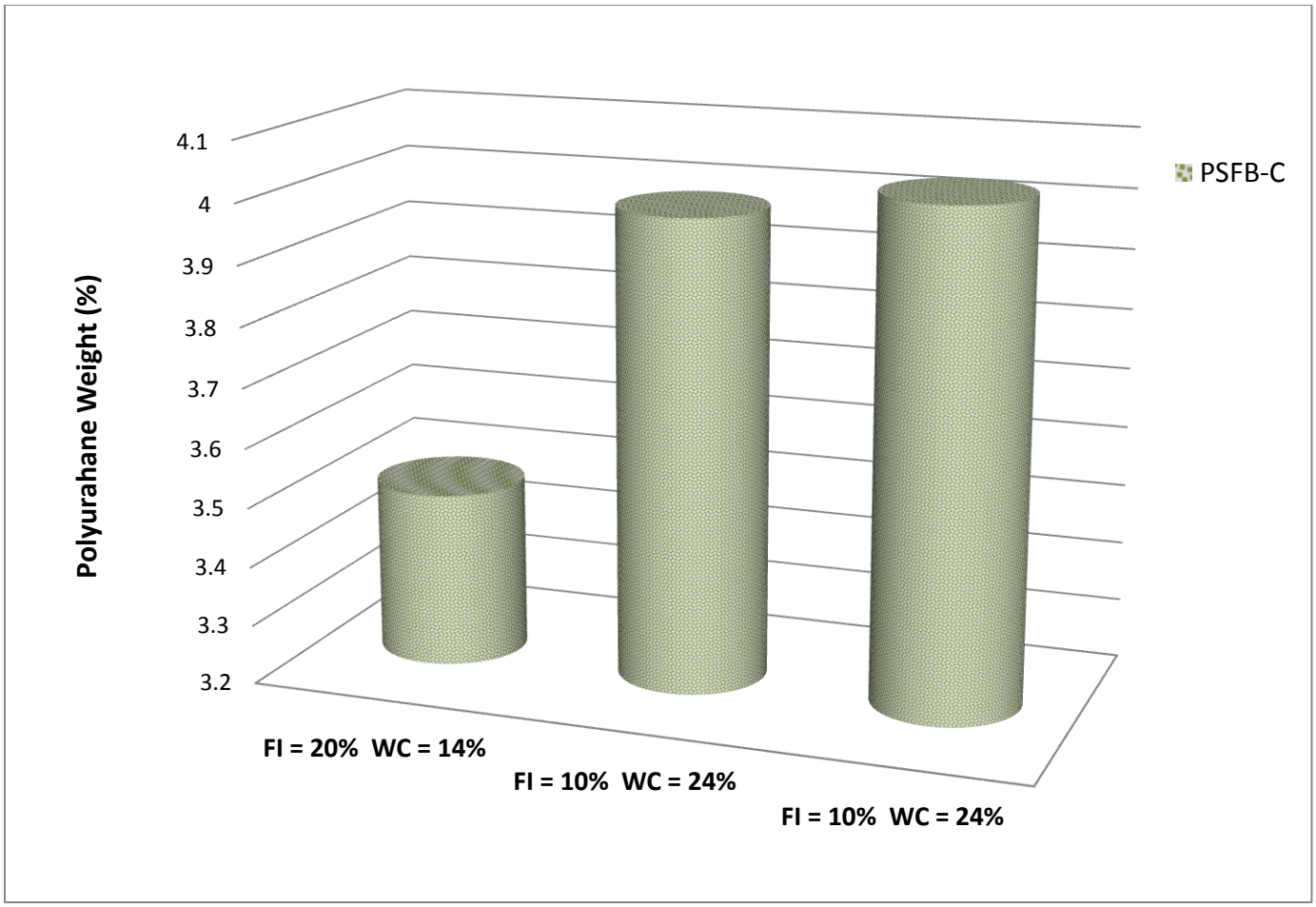

Figure 5.14 Percentage of Polyurethane Weight in PSFB-C with Different FI and WC

5.3.3 Polyurethane Stabilized Mineral Fouled Ballast (PSFB-M)

Mineral fouling is one of the non-cohesive fouling materials and the behavior of mineral fouling is similar to that of coal fouling, which is explained in section 5.3.1. The PSFB-M beam specimen (FI = 10% WC = 20 %) has the highest plastic strain of 0.97% (Fig.5.15). The impact of polyurethane stabilization in mineral fouled specimens was observed to be less than the other fouling types, but even after 500,000 cycles at 350 kPa deviator stress, the FRA maintenance limit of 2.5% - 3% was not exceeded. There was a mineral fouled ballast (FB-M) tested by Ebrahimi et al. (2011) that had a similar FI and WC (Fig. 5.16). After RPF injection procedure, mineral fouled ballast (FI = 10% WC = 20%) had its plastic strain decrease from 2.40% to 0.97%, which is 60% reduction. Table 5.4 shows the reduction of plastic strain of all PSFB-M to the unstabilized FB-M of Ebrahimi et al. (2011). Figure 5.17 shows that percentage of polyurethane weight in PSFB-M. The PSFB-M has lowest percentage of polyurethane weight with highest FI and WC, which filled between ballast particles and cause smaller voids in the ballast.

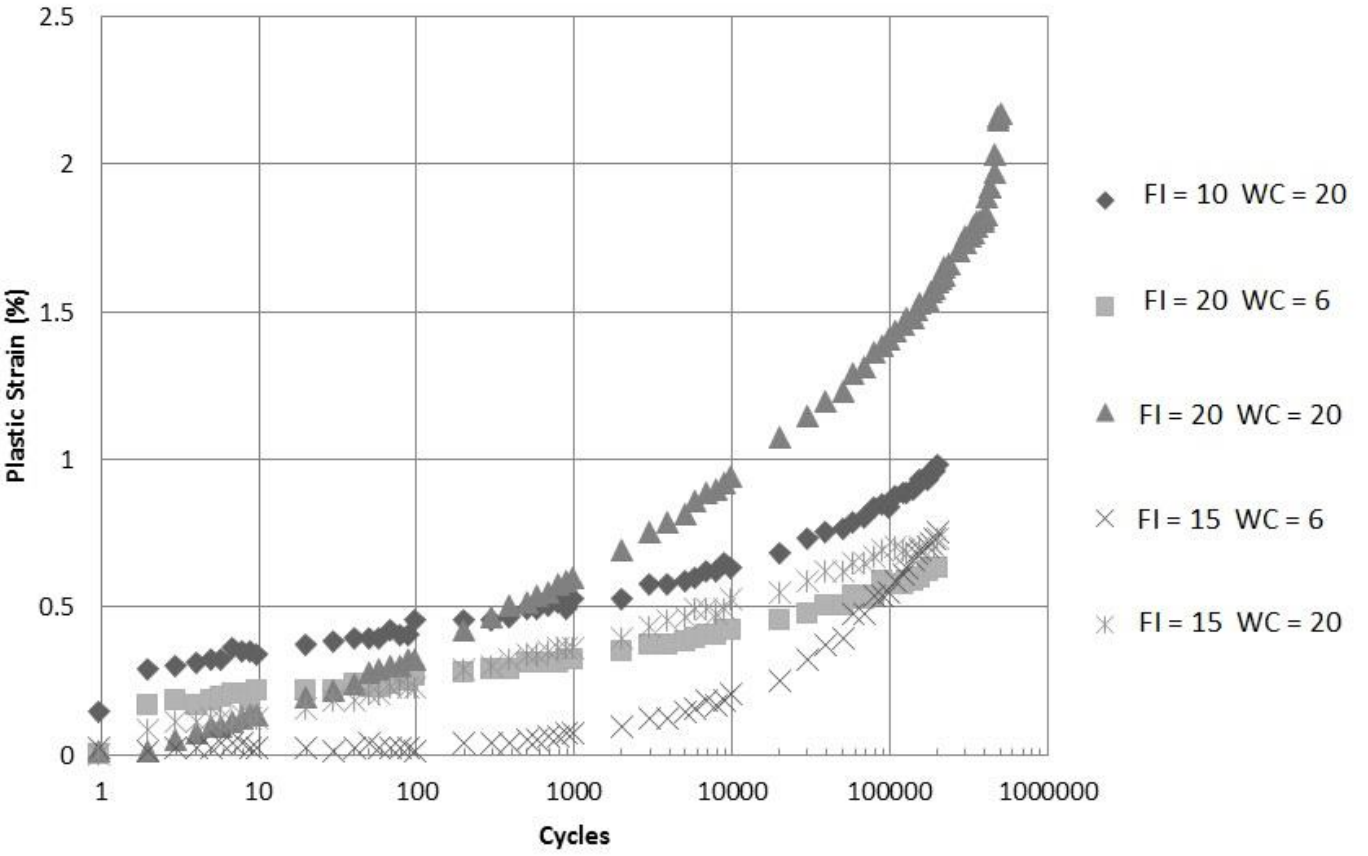

Figure 5.15 The Results of Large-Scale Cyclic - Triaxial Compression Tests on PSFB-M Specimens

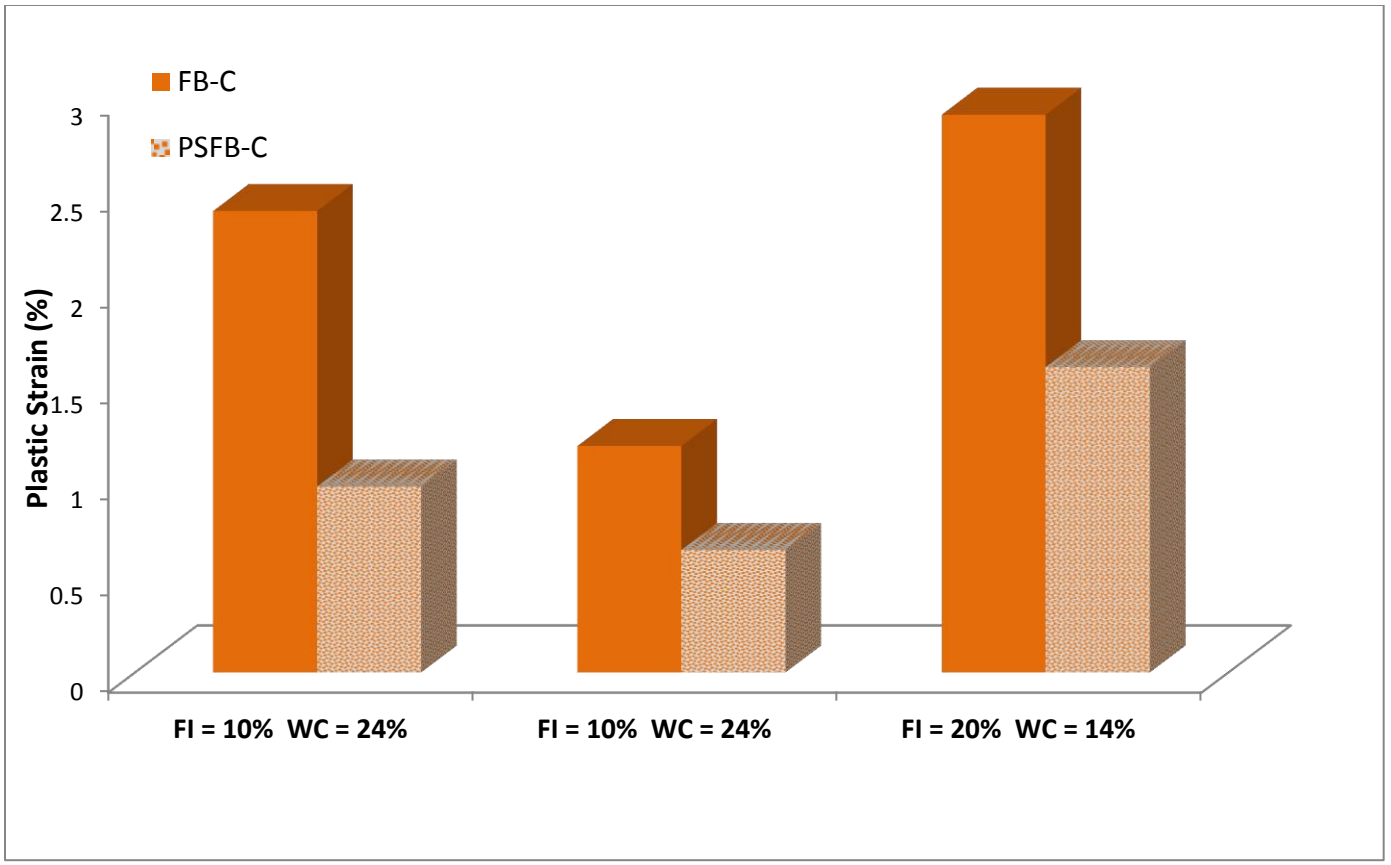

Figure 5.16 Plastic Strain Distribution Between PSFB-M and FB-M (Mineral Fouled Ballast) Over 200,000 Cycles

Table 5.4 Comparison of Plastic Strain Between PSFB-M and FB-M

Sample Description	**PSFB-M Plastic Strain**	**FB-M Plastic Strain** Ebrahimi et al. (2011)	**Reduction**
FI = 10% WC = 20%	0.97%	2.40%	60%
FI = 15% WC = 6%	0.75%	-	-
FI = 15% WC = 20%	0.73%	-	-
FI = 20% WC = 6%	0.64%	1.18%	46%
FI = 20% WC = 20%	1.59% *	2.9%	45%

*Equipment was not performing properly during this test, so this reading is artificially high

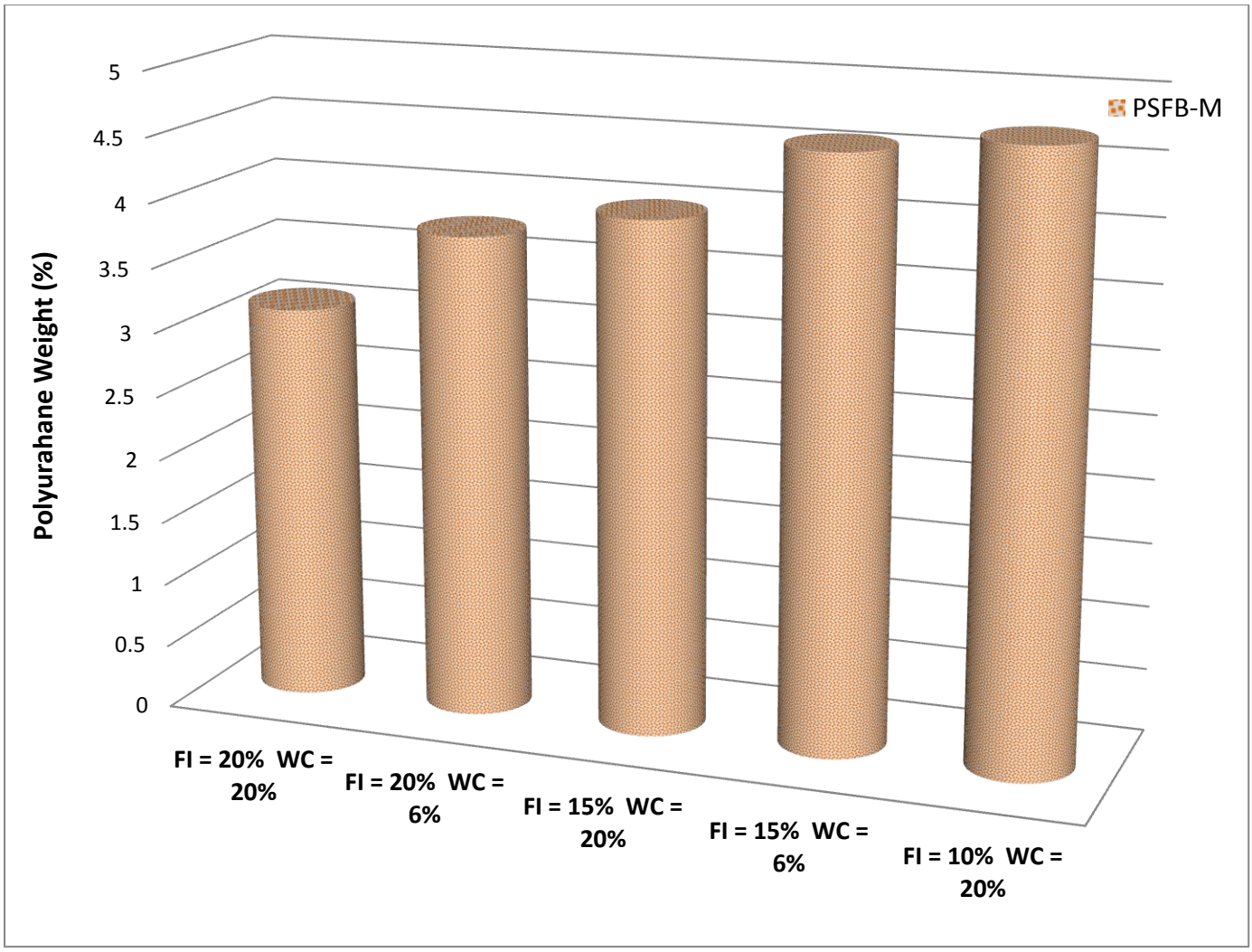

Figure 5.17 Percentage of Polyurethane Weight in PSFB-M with Different FI and WC

5.3.4 Polyurethane Stabilized Fouled with Fine Frac Sand (PSFB-F)

Two specimens with a specific FI and WC (i.e., FI = 24%, WC = 14%) were constructed with two ballast types. This was to examine whether ballast type influences the mechanical behavior of the PSFB matrix with coarse frac sand. The behavior seen in Figure 5.18 and summarized in Table 5.5 shows that, for the specimens of both types of ballast, the strain rates and the final deformation are approximately the same whether they are stabilized or not. Hesse (2014) conducted tests on unstabilized frac sand fouled ballasts also at 300 kPa deviator stress as here.

Table 5.5 Comparison of Plastic Strain Between PSFB-F and FB

Sample Description	**PSFB-F Plastic Strain**	**FB Plastic Strain Hesse (2013)***	**Reduction**
FI = 24% WC = 14% Dolomite	0.94%	1.50%	37%
FI = 24% WC = 14% Granite	0.88%	1.50%	41%

*The FI used in this comparison is 15%

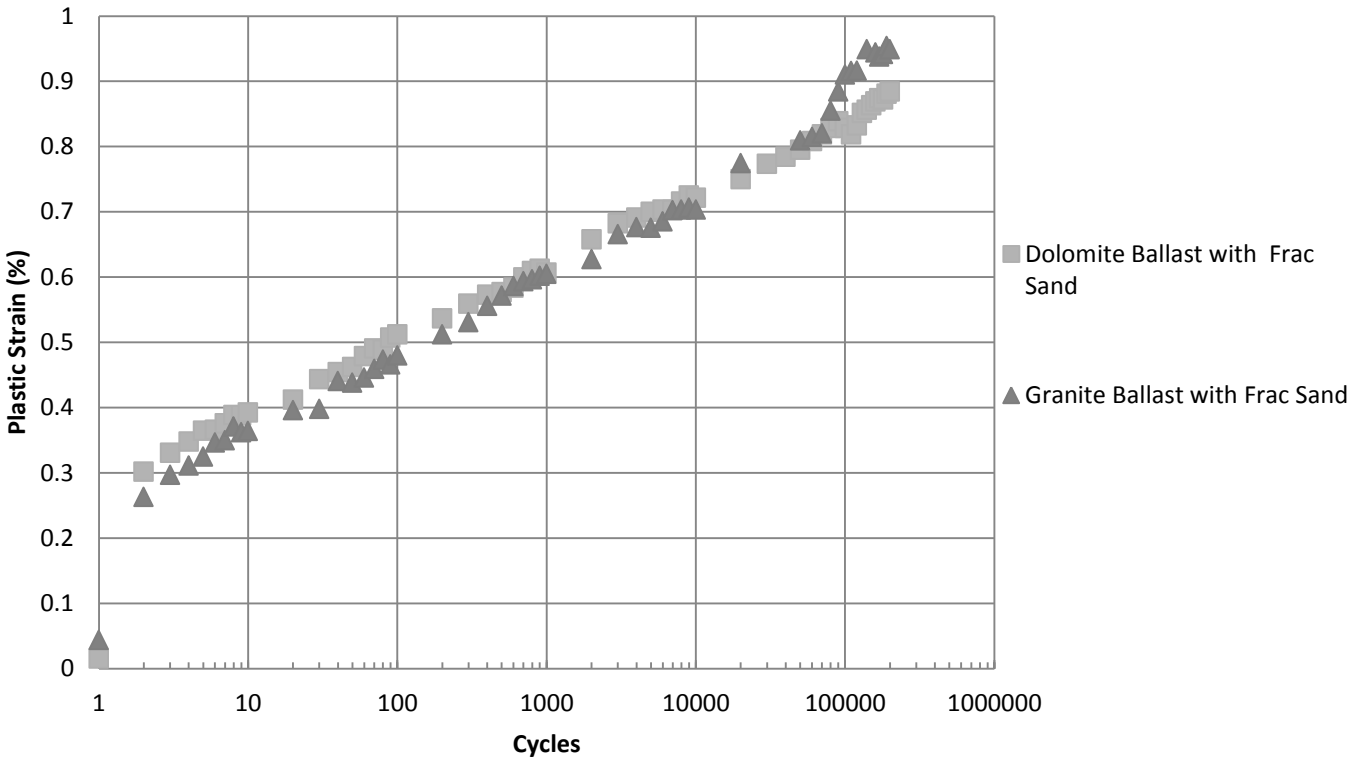

Figure 5.18 The Results of Large-Scale Cyclic-Triaxial Compression Testson PSFB-F Specimens

5.3.5 Comparison of Ballast Types

Replicates of specimens using granitic and dolomitic ballast were tested to see if ballast type has an influence on the RPF's ability to bond and decrease deformation. Table 5.6 shows the plastic strain comparison of the different types of ballast specimens with a variety of fouling metarials. The only large difference in behavior observed between the two ballast types was in the PSFB-M with a final plastic strain difference of 0.4%. That difference is attributed to heterogeneity of the specimens. The granite ballast specimen, at the top, had pockets of non-homogenous RPF foam and ballast.

Table 5.6 Comparison of Plastic Strains for Different Type of PSFB

Sample Description	**Dolomite Ballast**	**Granite Ballast**	**Difference**
PSFB-F	0.94%	0.88%	0.06%
PSFB-C	1.46%	1.30%	0.16%
PSFB-M	0.75%	1.15%	0.4%

The results were also compared with the results from PSB studied by Keene et al. (2012) and fouled ballast (FB) studied by Ebrahimi et al. (2011) as shown in Figure 5.19. The average plastic strain of the fouled ballast is the highest (2.6%) compare to the PSFB and PSB. The PSFB specimens have average ε_P of 77% less than the unstabilized fouled ballast. Furthermore, PSB specimens have average ε_P of 92% less than the fouled ballast. The PSB has 4.7 times less plastic strain ε_p than the fouled ballast. The main reason is that the percentage of the average volume of polyurethane in the PSFB is 0.47, whereas the percentage of the volume of polyurethane in PSB is 7.41, which is about 16 times higher. This clearly shows that the high amount of polyurethane significantly increases the resistance in the ballast.

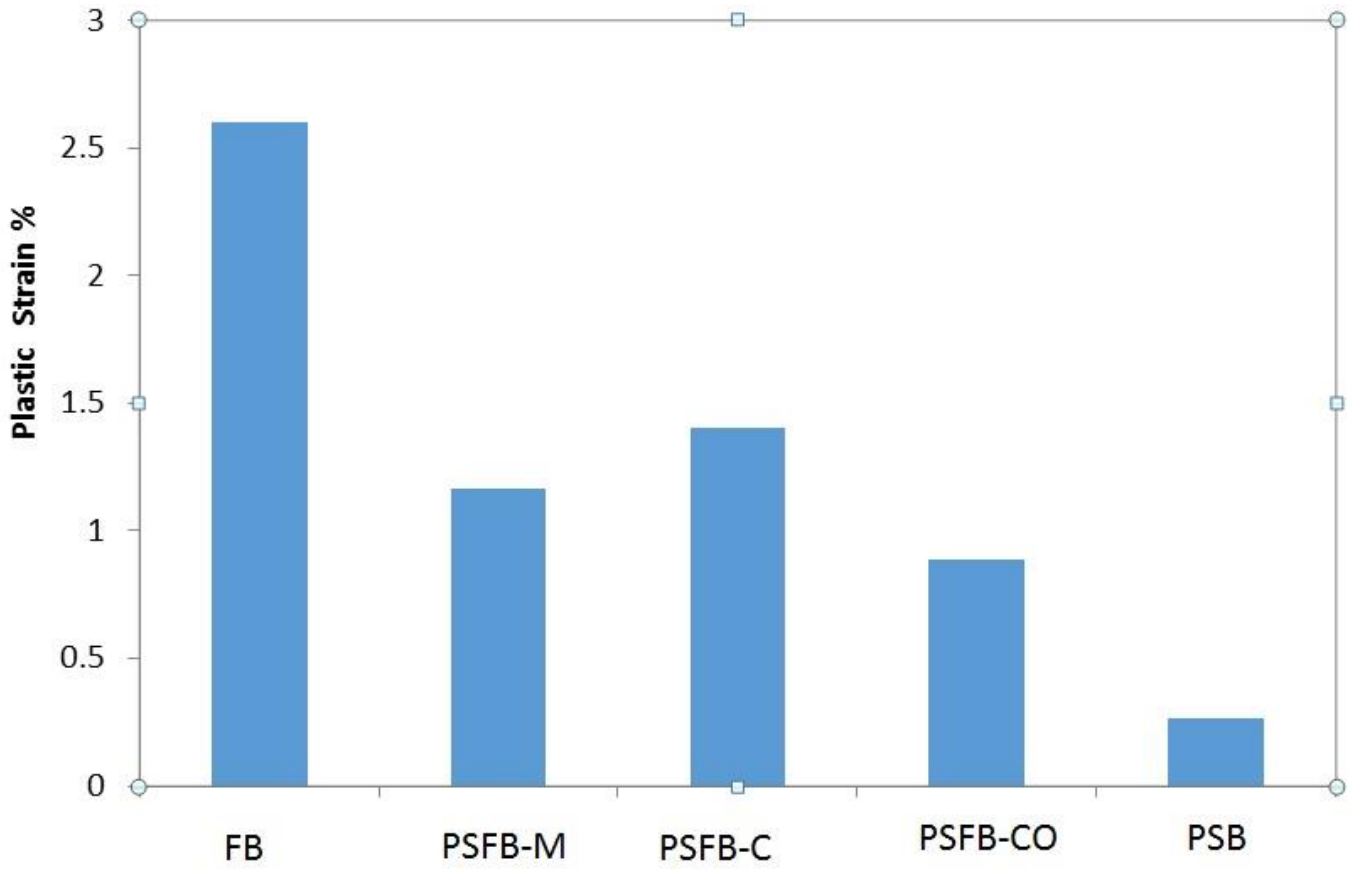

Figure 5.19 Large-Scale Cyclic Triaxial Compression Tests conducted on Fouling PSB with Different Fouling Indices (FI) and Water Contents (WC). The Results were Compared with PSB Keene et al. (2012) and Fouled Ballast Ebrahimi et al. (2011) Test Results.

To understand the deformational behavior of PSFB 19 cylindrical specimens were subjected to large-scale cyclic triaxial compression and seismic wave tests and 5 beam specimens in the monotonic flexural and unconfined-compression tests (UCS). The results indicate that PSFB has greater strength than clean unstabilized ballast and lower strength than PSB. The PSFB has lower strength than PSB because of the following reasons.

The first reason is that the mechanical behavior of PSFB and PSB are related to the percent rigid polyurethane foam (RPF) by weight in specimens. The PSB beam specimen (FI = 0% WC = 0%) has %5.4 RPF by weight and the PSFB beam specimen (FI = 15% WC = 13%) has only 3.4% RPF by weight (Table 5.7). PSB has 2% more polyurethane than PSFB.

The second reason is that polyurethane bonds well with ballast particles. The strength of the bonds between the ballast and the RPF, is similar to the mortar-aggregate bond in concrete. Behavior of concrete in compression is controlled by mortar-aggregate bond strength and aggregate-surface texture (Perry and Gillott 1997). They showed that unconfined compressive strength of concrete is greater with aggregates that are angular and with surfaces that are rough. For the dolomite ballast with e_B = 0.60, approximately 25% by weight of mineral fouling is required to contaminate all contact points; i.e., assuming that fully fouled ballast is achieved when all void space is filled with mineral fouling. With fouling indices of 10-25% (by weight), initially the specimens had about 50%-100% of their contact points fouled before RPF injection. The bonding properties are unique due to the interaction of the polyurethane with the aggregates. Coated ballast with fouling material and water does not bond well with polyurethane during the RPF reaction (Fig. 5.20).

The third reason is that the presence of FI can result in heterogeneous polyurethane distribution in the specimen since the polyurethane push to the fouling material during to expansion time resulting in two different regions in the ballast specimen (see Fig. 5.21).

Table 5.7 Distribution of RPF in PSFB and PSB Beams

Beams FI and WC	RPF Weight (%)	RPF Weight (lbs)
FI = 15% - WC = 8%	3.5	4.65
FI = 10% - WC = 13%	3.9	4.92
FI = 10% - WC = 8%	4.2	5.17
FI = 15% - WC = 13%	3.4	4.43
FI = 0% - WC = 0%	5.4	6.14

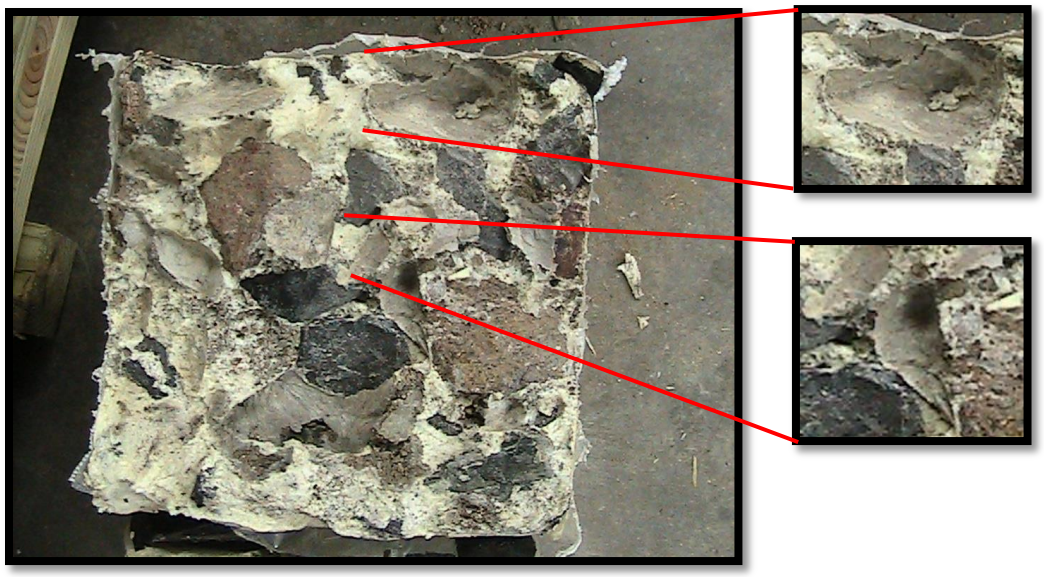

Figure 5.20 Pictures of PSFB after Monotonic Flexural Test

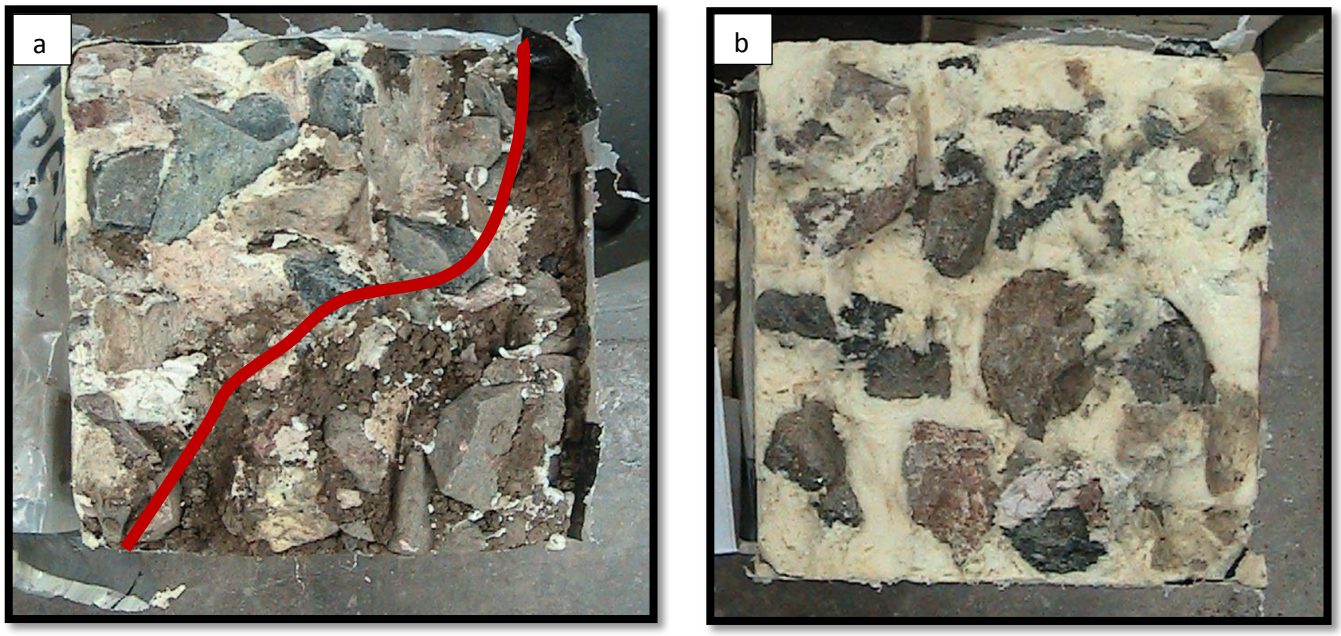

Figure 5.21 Pictures of PSFB (a) and PSB (b)

5.4 Elastic-Wave Test Results

Elastic wave (seismic) tests were conducted on PSFB specimens before and after cyclic triaxial testing and compared to the results obtained from cyclic-triaxial compression testing on the same specimens. The constrained modulus (M) was calculated as follows;

$$M = V_p^2 \rho_B \qquad \text{Eq. (5.7)}$$

where V_p is p-wave velocity (m/s), ρ_B is the bulk density of PSFB (kg/m^3). The results indicated that the constrained modulus is a function of specimen density and significantly decreases after the cyclic-triaxial loading of the specimen. Before cyclic-triaxial compression test, cylindrical PSFB-C (FI = 24 WC = 14) constrained modulus was 345 MPa. After 200,000 loading cycles, cylindrical constrained modulus was 245 MPa. Elastic wave testing conducted for specimen damage detection exhibits that the higher density PSFB specimen has a greater resistance to accumulation of plastic strain from cyclic-triaxial compression tests than the lower density PSFB specimen. Finally, percent polyurethane (RPF) by weight was higher in the denser specimen and correspondingly lower in the less dense specimen. Comparison of constraint modulus between PSFB specimens before and after cyclic-triaxial compression tests can be seen in following Figure 5.22.

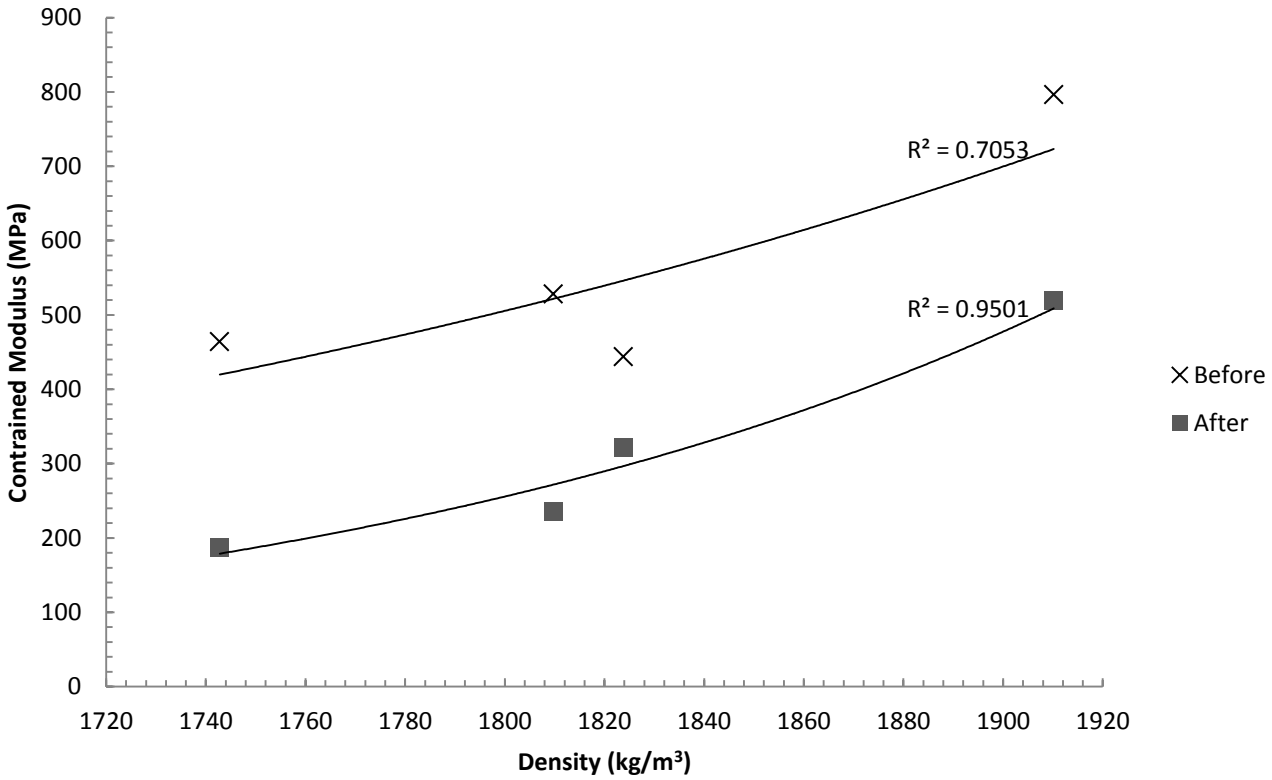

Figure 5.22 Comparison of Constraint Modulus Between PSFB Specimens Before and After Cyclic-Triaxial Compression Tests

7. CONCLUSIONS

In this study 19 PSFB cylindrical samples, which had different FI and WC and four PSFB and one PSB beam samples were tested under cyclic triaxial with seismic (cylinders), and monotonic flexural and unconfined compression tests (beams).

Monotonic-flexural testing is used for determining flexural strength of bound materials that undergo bending stresses in transportation infrastructure. The PSB beam specimen (FI = 0% WC = 0%) has the highest flexural strength (rupture modulus) of 1582 kPa while the PSFB specimen with the highest fouling (FI = 15%) and water content (WC = 13%) has the lowest flexural strength of 311 kPa. The PSB flexural strength is approximately five times greater than highest fouled PSFB sample.

Unconfined compressive strength (UCS) testing is typically used for determining strength and Young's modulus of materials as a reference index to verify that other mechanical properties can be confirmed in the material. UCS test results show that the highest unconfined compression strength of 2850 kPa was reached by the PSB (FI = 0% WC = 0%). Highest fouling (FI = 15%) and water content (WC = 13%) in the PSFB yielded strength around 1763 kPa. Reference clean ballast is unstabilized and because angular mineral particle contacts are present a higher elastic modulus than PSFB and PSB occurs. After the RPF injection procedure, the clean ballast elastic modulus decreases from 275 MPa to 98 MPa as polyurethane enters the ballast particle contacts. PSFB has higher elastic modulus than PSB because of high percentage of polyurethane weight in PSB.

Cyclic triaxial compression testing is used for determining plastic deformational behavior of infrastructure materials commonly exposed to repetitive compressive loading in the field. Initial cyclic triaxial tests were conducted at a deviator stress, σ_d, of 350 kPa, PSFB deformational behavior varied as RPF density varied. The PSFB specimens have average final ε_P 77% less than the unstabilized fouled ballast counterparts. Furthermore, PSB specimens have average ε_P of 92% less than the clean unstabilized ballast. It is noted that after 200-500 thousand loading cycles, none of the polyurethane stabilized specimens went over the recommended maintenance limit of 2.5% - 3% by the FRA.

Based on the test results of this research, the injection of polyurethane into fouled ballast proves to be an effective method of reducing plastic strain and increasing strength. Polyurethane stabilized fouled ballast (PSFB) displays superior mechanical behavior in comparison to fouled ballast without polyurethane stabilization. As the amount of fouling material increases, the strength decreases. As water content increases there is a decrease in strength as well. The polyurethane injection method replicated in the fouled ballast did not result in a composite material as strong as PSB. The first reason is that fouling interacts with the contact points of ballast particles which reduces the shear resistance properties of the ballast skeleton and accelerates the accumulation of plastic strain. The second reason is when fouling material coats the surface of ballast the polyurethane does not bond well with ballast particles during the RPF reaction. Another reason is when the fouling material becomes wet, excess pore water pressure develops between fine particles resulting in a weaker ballast structure. Last reason is that when fouling materials fills the ballast voids it leaves smaller voids available to be filled with RPF. On the other hand, polyurethane injection methods reduce plastic strain and increase

strength. After the injection, the polyurethane fills ballast voids and prevents: (1) ballast particle breakage, (2) relocation of ballast particles, (3) friction wear of particles.

8. REFERENCES

Anderson, W.F. & Fair, P. (2008). “Behavior of Railroad Ballast under Monotonic and Cyclic Loading.” Journal of Geotechnical and Geoenvironmental Engineering, ASCE, 134(3), 316–328.

Aursudkij, A., McDowell, G.R., Collop, A.C. (2009). “Cyclic Loading of Railway Ballast Under Triaxial Conditions and In A Railway Test Facility.” Granular Matter, (11), 391–401.

Bayer Material Science (2010). 486STAR Polyurethane Foam Grout. Technical Data Sheet, Spring, Texas.

Becker, R. and Patrick, V. (2005). “Integral Ballast Recycling to Sustainable Development.” Railway Gazette International, 161(1), 44–46.

164

Bishop, A.W. & Green, G.E. (1965). “The Influence of End Restraint on the Compression Strength of a Cohesionless Soil.” Geotechnique, (15), 243–266.

Chrismer, S. & Davis, D. (2000). "Cost Comparisons of Remedial Methods to Correct Track Substructure Instability." Transportation Research Record, 1713 (00-019), 10-15.

Dersch, M.S., Tutumluer, E., Peeler, C.T., & Bower, D.K. (2010). "Polyurethane Coating of Railroad Ballast Aggregate for Improved Performance." Proceedings of the Joint Rail Conference, April 27-29, 2010, Urbana, IL, USA.

Ebrahimi, A. (2011). “Deformational Behavior of Fouled Railway Ballast.” PhD thesis, Department of Civil and Environmental Engineering, University of Wisconsin, Madison.

Ebrahimi et al. (2011) “Protocol for Testing Fouled Railway Ballast in Large-Scale Cyclic Triaxial Equipment,” ASTM Geotechnical Testing Journal, (ASTM GTJ103846)

Erdemgil, M., Sağlam, S., & Bakır, B.S. (2007). “Utilization of highly expansive polymer injection to mitigate seismic fou(ndation for existing structures.” 8th Pacific Conference on Earthquake Eng., December 5-7, 2007, Singapore.

Freitas, S.T., Kolstein, H., & Bijlaard, F. (2010). "Parametric Study of the Interface Layer Renovation for Orthotropic Steel Bridge Decks." Computer-Aided Civil and Infrastructure Engineering, 27, 143–153.

Huang, H., Shen, S., & Tutumluer, E. (2009). "Sandwich Model to Evaluate Railroad Asphalt Trackbed Performance Under Moving Loads." Transportation Research Record, No. 2117, 57–65.

Lichtberger, B. (2005). Track Compendium – Formation, Permanent Way, Maintenance, Economics. Eurail Press, Hamburg, Germany.

Perry, C. & Gilliott, J.E. (1977). "The Influence of Mortar-Aggregate Bond Strength on The Behaviour of Concrete in Uniaxial Compression." Cement and Concrete Research: Pergamon Press, Inc. Elmsford, NY, 7, 553–564.

Polito, C.P., and Martin II, J.R., 2001, Effects of Nonplastic Fines on the Liquefaction Resistance of Sands, J. of Geotech. & Geoenviron. Eng., ASCE, 127(5), pp.408–415

Randall, D. & Lee, S. (2002). The Polyurethanes Book. John Wiley and Sons LTD., West Sussex, England.

Rudolf, B. & Vierlinger, P. (2005). "Integral ballast recycling contributes to sustainable development." Railway Gazette International, 161, 44–46.

Selig, E.T. & Waters, J.M. (1994). Track Geotechnology and Substructure Management.

Skempton, A.W. (1954). "The pore pressure coefficients A and B". Geotechnique, 4(4), 143-147Thomas Telford, New York, NY.

Skoglund, K.A. (2002). "A study of some factors in mechanistic railway track design." PhD thesis, Norwegian University of Science and Technology.

Wisconsin & Southern Railroad. (2002). Satisfying customers needs through continuous improvements. Wisconsin & Southern Railroad.

Woodward, P.K., Thomson, D., & Bahimahd, M. (2007). "Geocompostie Technology: Reducing Railway Maintenance." Proceedings of the Institute of Civil Engineers, (TR3), 109–115.